A SPATIAL-TEMPORAL ASYMPTOTIC PRESERVING SCHEME FOR RADIATION MAGNETOHYDRODYNAMICS

SHI JIN, MIN TANG, AND XIAOJIANG ZHANG

Abstract. The radiation magnetohydrodynamics (RMHD) system couples the ideal magnetohydrodynamics equations with a gray radiation transfer equation. The main challenge is that the radiation travels at the speed of light while the magnetohydrodynamics changes with fluid. The time scales of these two processes can vary dramatically. In order to use mesh sizes and time steps that are independent of the speed of light, asymptotic preserving (AP) schemes in both space and time are desired. In this paper, we develop an AP scheme in both space and time for the RMHD system. Two different scalings are considered, one results in an equilibrium diffusion limit system, while the other results in a non-equilibrium system. The main idea is to decompose the radiative intensity into three parts, each part is treated differently. The performances of the semi-implicit method are presented, for both optically thin and thick regions, as well as for the radiative shock problem. Comparisons with the semi-analytic solution are given to verify the accuracy and asymptotic properties of the method.

1. Introduction

Radiation magnetohydrodynamics (RMHD) is concerned about the dynamical behaviors of magnetized fluids that have nonnegligible exchange of energy and momentum with radiation, which is important in high temperature flow systems, solar and space physics and astrophysics. The radiation transfer equation (RTE) for the radiative intensity I and the fluid temperature T in the mixed frame is governed by

$$\begin{aligned}\frac{\partial I}{\partial t}+C\boldsymbol{n}\cdot\nabla I=C\sigma_a\left(\frac{a_rT^4}{4\pi}-I\right)+C\sigma_s(J-I)+3\boldsymbol{n}\cdot\boldsymbol{v}\sigma_a\left(\frac{a_rT^4}{4\pi}-J\right)+\boldsymbol{n}\cdot\boldsymbol{v}(\sigma_a+\sigma_s)(I+3J)\\-2\sigma_s\boldsymbol{v}\cdot\boldsymbol{H}-(\sigma_a-\sigma_s)\frac{\boldsymbol{v}\cdot\boldsymbol{v}}{C}J-(\sigma_a-\sigma_s)\frac{\boldsymbol{v}\cdot(\boldsymbol{v}\cdot K)}{C},\end{aligned}\tag{1.1}$$

where σ_a and σ_s represent absorption and scattering opacities respectively, $\boldsymbol{n}\in V$ is the angular variable, a_r is the radiation constant and C is the speed of light [7]. The ideal MHD equations with radiation energy and momentum source terms are

$$\begin{cases}\dfrac{\partial\rho}{\partial t}+\nabla\cdot(\rho\boldsymbol{v})=0,\\ \dfrac{\partial(\rho\boldsymbol{v})}{\partial t}+\nabla\cdot(\rho\boldsymbol{v}\boldsymbol{v}-\boldsymbol{B}\boldsymbol{B}+P^*)=-\boldsymbol{S_{rp}},\\ \dfrac{\partial E}{\partial t}+\nabla\cdot[(E+P^*)\boldsymbol{v}-\boldsymbol{B}(\boldsymbol{B}\cdot\boldsymbol{v})]=-CS_{re},\\ \dfrac{\partial\boldsymbol{B}}{\partial t}+\nabla\times(\boldsymbol{v}\times\boldsymbol{B})=0\,,\end{cases}\tag{1.2}$$

where

$$S_{re}=\sigma_a(a_rT^4-E_r)+(\sigma_a-\sigma_s)\frac{\boldsymbol{v}}{C^2}\cdot\left[\boldsymbol{F_r}-(\boldsymbol{v}E_r+\boldsymbol{v}\cdot P_r)\right],$$

$$\boldsymbol{S_{rp}}=-\frac{\sigma_s+\sigma_a}{C}\left[\boldsymbol{F_r}-(\boldsymbol{v}E_r+\boldsymbol{v}\cdot P_r)\right]+\frac{\boldsymbol{v}}{C}\sigma_a(a_rT^4-E_r),$$

Date: January 12, 2021.

with the energy density

$$E_r = 4\pi J = \frac{4\pi}{|V|}\int_V I \mathrm{d}\boldsymbol{n} = 4\pi \langle I \rangle ,$$

the radiation flux

$$\boldsymbol{F_r} = 4\pi C \boldsymbol{H} = \frac{4\pi C}{|V|}\int_V \boldsymbol{n} I \mathrm{d}\boldsymbol{n} = 4\pi C \langle \boldsymbol{n} I \rangle ,$$

and the radiation pressure

$$P_r = 4\pi K = \frac{4\pi}{|V|}\int_V \boldsymbol{n}^2 I \mathrm{d}\boldsymbol{n} = 4\pi \langle \boldsymbol{n}^2 I \rangle .$$

In particular, the operators $\langle \cdot \rangle$, $\langle \boldsymbol{n}\cdot \rangle$ and $\langle \boldsymbol{n}^2\cdot \rangle$ are respectively $\frac{1}{|V|}\int_V \cdot \mathrm{d}\boldsymbol{n}$, $\frac{1}{|V|}\int_V \boldsymbol{n}\cdot \mathrm{d}\boldsymbol{n}$ and $\frac{1}{|V|}\int_V \boldsymbol{n}^2\cdot \mathrm{d}\boldsymbol{n}$ in context. Moreover, ρ is fluid density, $\boldsymbol{v}$ is fluid velocity, $\boldsymbol{B}$ is magnetic flux density, p is static pressure, P^* is full pressure of fluid, $P^* \equiv (p + B^2/2)\mathrm{M}$ (with M the unit tensor), and the total fluid energy density is

$$E = E_g + \frac{1}{2}\rho v^2 + \frac{B^2}{2},$$

where E_g is the internal energy density, $v^2 = \boldsymbol{v}\cdot\boldsymbol{v}$ and $B^2 = \boldsymbol{B}\cdot\boldsymbol{B}$. The radiation MHD system is closed by the perfect gas equation of state:

$$E_g = p/(\gamma - 1), \qquad T = p/(R_{\mathrm{ideal}}\rho),$$

where γ is adiabatic index for an ideal gas, and R_{ideal} is the ideal gas constant.

Numerical approximations to RTE have been extensively studied in [12,14,15,21,24,30] and for ideal MHD see for example [2,18,29]. The RMHD coupled system has been investigated lately [1,6,7,13,27,28,31]. Since the transport term in the RTE and the advection term in the MHD equations are at different time scales, the RMHD system can be stiff, as can been seen more clearly after nondimensionalization [19]. To solve the RMHD system, classical numerical discretizations require the space and time steps resolve the speed of light, which leads to very expensive computational cost. Asymptotic-Preserving (AP) schemes provide a generic framework for such multiscale problems [8,9]. AP schemes were first studied for steady neutron transport problems in diffusive regimes [16,17] and then [5,10] for boundary value problems, and unsteady transport problems [11,14]. In the discrete setting, from the microscopic scale to the macroscopic, AP schemes preserve the asymptotic limit. When the scaling parameter ε in the multiscale system can not be resolved numerically, AP schemes should automatically become a good solver for the macroscopic models.

AP schemes for RMHD have been proposed in the literature but since most of them are based on operator splitting, they are only AP in space. In [1], Simon et al. have developed a second-order scheme in both space and time for the Euler equations coupled with a gray radiation S_2 model. The scheme in [1] uses MUSCL-Hancock method to solve the Euler equations and the lumped linear-discontinuous Galerkin method for the radiation S_2 model. For the time discretization, the TR/BDF2 time integration method is employed. Jiang et al. devised an Implicit/Explicit (IMEX) scheme for the splitting system that treats the transport term in the RTE and convective term in the fluid equations explicitly, and the source term implicitly [7]. Recently, another method by Sun etc. [31] uses the gas-kinetic scheme (GKS) to deal with Euler equations and the unified gas-kinetic scheme (UGKS) for the RTE. However, all the aforementioned methods either require a time step that satisfies a hyperbolic constraint with CFL number proportional to the light speed [1,7], or use nonlinear iterations involving (1.1) in order to get rid of the time step constraint [31]. Both approaches are expensive. It is desired to design a scheme that can use a time step that is independent of the light speed and employs nonlinear iterations that involve only macroscopic quantities, i.e. the ρ, $\boldsymbol{v}$, E, $\boldsymbol{B}$ or the moments of radiative intensity.

In this paper, we aim at developing a scheme for RMHD that is AP in *both* space *and* time. Two different parameter regimes are considered. One is for σ_a small and σ_s large, which results in the non-equilibrium diffusion limit system. The other is for σ_a large, which gives the equilibrium diffusion limit system. The proposed scheme preserves both limits. The main idea is to decompose the intensity into three parts, two parts correspond to the zeroth and first order moments, while the third part is the residual. The two macroscopic moments are treated implicitly while the residual is explicit. Thanks to the properties of residual term, one can update the macroscopic quantities first. For the space discretization, we use Roe's method in the Athena code to solve the convective part in the ideal MHD equations and the UGKS for the RTE. AP property of both semi-discretized and fully discretizad are proved.

This paper is organized as follows. Section 2 gives the asymptotic limit of the coupled system, and the equilibrium and non-equilibrium diffusion limit systems under different scalings are obtained. The semi-discretization and one dimensional fully discretized scheme for RMHD are illustrated in Sections 3 and 4 respectively. Their capability of capturing both diffusion limits are proved. In Section 5, performances of our AP method are presented in both optically thin and thick regions. The radiative shock problems are tested. By comparing with the semi-analytic solutions in [20], we observe that the scheme is accurate and stable using large time step and meshes that are independent of the light speed. Finally, we conclude in Section 6.

2. The diffusion limit of RMHD

As presented in [19], the dimensionless form for the coupled system can give a better insight on the relative importance of different terms. Consider the following nondimensionalization:

$$x = \widehat{x}\ell_\infty, \quad t = \widehat{t}\ell_\infty/a_\infty, \quad \rho = \widehat{\rho}\rho_\infty, \quad \boldsymbol{v} = \widehat{\boldsymbol{v}}a_\infty, \quad p = \widehat{p}\rho_\infty a_\infty^2, \quad T = \widehat{T}T_\infty, \quad I = a_r T_\infty^4 \widehat{I},$$
$$E_r = a_r T_\infty^4 \widehat{E_r}, \quad \boldsymbol{F_r} = C a_r T_\infty^4 \widehat{\boldsymbol{F_r}}, \quad P_r = a_r T_\infty^4 \widehat{P_r}, \quad \sigma_a = \lambda_a \widehat{\sigma_a}, \quad \sigma_s = \lambda_s \widehat{\sigma_s},$$

where variables with a hat denote nondimensional quantity and variables with $\infty-$subscript are the characteristic value with unit. More precisely, ℓ_∞, a_∞, ρ_∞ and T_∞ are respectively the reference length, sound speed, density and temperature. Moreover, λ_a and λ_s are respectively the characteristic value of absorbing and scattering coefficients. Then the full dimensionless radiation MHD system becomes

$$\begin{cases} \dfrac{\partial I}{\partial t} + \mathcal{C}\boldsymbol{n}\cdot\nabla I = \mathscr{L}_a\mathcal{C}\sigma_a\left(\dfrac{T^4}{4\pi} - I\right) + \mathscr{L}_s\mathcal{C}(J-I) + 3\mathscr{L}_a\boldsymbol{n}\cdot\boldsymbol{v}\sigma_a\left(\dfrac{T^4}{4\pi} - J\right) + \boldsymbol{n}\cdot\boldsymbol{v}\left(\mathscr{L}_a\sigma_a + \mathscr{L}_s\sigma_s\right)(I+3J) \\ \qquad - 2\mathscr{L}_s\sigma_s\boldsymbol{v}\cdot\boldsymbol{H} - (\mathscr{L}_a\sigma_a - \mathscr{L}_s\sigma_s)\dfrac{\boldsymbol{v}\cdot\boldsymbol{v}}{\mathcal{C}}J - (\mathscr{L}_a\sigma_a - \mathscr{L}_s\sigma_s)\dfrac{\boldsymbol{v}\cdot(\boldsymbol{v}\cdot K)}{\mathcal{C}} \triangleq \mathcal{C}S, \\ \dfrac{\partial \rho}{\partial t} + \nabla\cdot(\rho\boldsymbol{v}) = 0, \\ \dfrac{\partial(\rho\boldsymbol{v})}{\partial t} + \nabla\cdot(\rho\boldsymbol{v}\boldsymbol{v} - \boldsymbol{B}\boldsymbol{B} + P^*) = -\mathcal{P}_0\boldsymbol{S_{rp}}, \\ \dfrac{\partial E}{\partial t} + \nabla\cdot[(E+P^*)\boldsymbol{v} - \boldsymbol{B}(\boldsymbol{B}\cdot\boldsymbol{v})] = -\mathcal{C}\mathcal{P}_0 S_{re}, \\ \dfrac{\partial \boldsymbol{B}}{\partial t} + \nabla\times(\boldsymbol{v}\times\boldsymbol{B}) = 0\,, \end{cases} \tag{2.1}$$

where $\mathcal{C} = \frac{C}{a_\infty}$, $\mathcal{P}_0 = \frac{a_r T_\infty^4}{\rho_\infty a_\infty^2}$, $\mathscr{L}_a = \ell_\infty\lambda_a$, $\mathscr{L}_s = \ell_\infty\lambda_s$, $S_{re} = 4\pi\langle S\rangle$ and $\boldsymbol{S_{rp}} = 4\pi\langle\boldsymbol{n}S\rangle$. In (2.1), $\mathcal{P}_0$ is a nondimensional constant, which measures the influence of radiation on the flow dynamics. In [4], the authors considered the equilibrium diffusion regime and non-equilibrium diffusion regime for a simplified coupled system. In the subsequent part, we consider the equilibrium diffusion limit and non-equilibrium diffusion limit of the RMHD system by using the same scaling assumptions as in [4].

2.1. **The non-equilibrium diffusion limit.**

In the simulation of radiation-hydrodynamics in [1], the speed of light $C = 29.98$ $cm\ ns^{-1}$, in nonrelativistic flows the sound speed is 0.001386 $cm\ ns^{-1}$, the radiation constent $a_r = 0.001372$ $Jk\ cm^{-3}\ KeV^{-4}$, the typical computational domain is 0.04 cm, and the units of the length, time, temperature and energy are respectively cm, ns, KeV and Jk. Therefore $1/\mathcal{C} = \mathcal{O}(\varepsilon)$, $\mathcal{P}_0 = \mathcal{O}(1)$. In non-equilibrium regime, we assume $\mathscr{L}_a = \varepsilon, \mathscr{L}_s = 1/\varepsilon$, and the radiation intensity I tends to a state which can be characterized by a temperature which is different from the material temperature T. In summary, we consider the following scaling

$$\mathscr{L}_a = \varepsilon, \quad \mathscr{L}_s = 1/\varepsilon, \quad \mathcal{P}_0 = \mathcal{O}(1), \quad \mathcal{C} = c/\varepsilon.$$

The RMHD system (2.1) becomes (after dropping the hat):

$$\begin{cases} \dfrac{\partial I}{\partial t} + \dfrac{c}{\varepsilon}\boldsymbol{n}\cdot\nabla I = c\sigma_a\left(\dfrac{T^4}{4\pi} - I\right) + \dfrac{c\sigma_s}{\varepsilon^2}(J-I) + 3\varepsilon\boldsymbol{n}\cdot\boldsymbol{v}\sigma_a\left(\dfrac{T^4}{4\pi} - J\right) + \boldsymbol{n}\cdot\boldsymbol{v}\left(\varepsilon\sigma_a + \dfrac{\sigma_s}{\varepsilon}\right)(I+3J) \\ \qquad\qquad -2\dfrac{\sigma_s}{\varepsilon}\boldsymbol{v}\cdot\boldsymbol{H} - (\varepsilon^2\sigma_a - \sigma_s)\dfrac{\boldsymbol{v}\cdot\boldsymbol{v}}{c}J - (\varepsilon^2\sigma_a - \sigma_s)\dfrac{\boldsymbol{v}\cdot(\boldsymbol{v}\cdot K)}{c}, & (2.2a) \\ \dfrac{\partial \rho}{\partial t} + \nabla\cdot(\rho\boldsymbol{v}) = 0, & (2.2b) \\ \dfrac{\partial(\rho\boldsymbol{v})}{\partial t} + \nabla\cdot(\rho\boldsymbol{v}\boldsymbol{v} - \boldsymbol{B}\boldsymbol{B} + P^*) = -\mathcal{P}_0\boldsymbol{S_{rp}}, & (2.2c) \\ \dfrac{\partial E}{\partial t} + \nabla\cdot[(E+P^*)\boldsymbol{v} - \boldsymbol{B}(\boldsymbol{B}\cdot\boldsymbol{v})] = -\dfrac{c}{\varepsilon}\mathcal{P}_0 S_{re}, & (2.2d) \\ \dfrac{\partial \boldsymbol{B}}{\partial t} + \nabla\times(\boldsymbol{v}\times\boldsymbol{B}) = 0\,, & (2.2e) \end{cases}$$

where

$$S_{re} = \varepsilon\sigma_a\left(T^4 - \frac{4\pi}{|V|}\int_V I\mathrm{d}\boldsymbol{n}\right) + (\varepsilon^3\sigma_a - \varepsilon\sigma_s)\frac{4\pi\boldsymbol{v}}{c^2|V|}\cdot\left[\frac{c}{\varepsilon}\int_V \boldsymbol{n}I\mathrm{d}\boldsymbol{n} - \left(\boldsymbol{v}\int_V I\mathrm{d}\boldsymbol{n} + \boldsymbol{v}\int_V \boldsymbol{n}^2 I\mathrm{d}\boldsymbol{n}\right)\right],$$

$$\boldsymbol{S_{rp}} = -\frac{4\pi(\sigma_s + \varepsilon^2\sigma_a)}{c|V|}\left[\frac{c}{\varepsilon}\int_V \boldsymbol{n}I\mathrm{d}\boldsymbol{n} - \left(\boldsymbol{v}\int_V I\mathrm{d}\boldsymbol{n} + \boldsymbol{v}\int_V \boldsymbol{n}^2 I\mathrm{d}\boldsymbol{n}\right)\right] + \frac{\boldsymbol{v}}{c}\varepsilon^2\sigma_a\left(T^4 - \frac{4\pi}{|V|}\int_V I\mathrm{d}\boldsymbol{n}\right).$$

When $\varepsilon \to 0$, we show that the solution to (2.2) can be approximated by the solution to a nonlinear diffusion equation coupled with a MHD system. We assume that the radiation intensity I and temperature T have the following Chapman-Enskog expansion such that

$$\begin{aligned} I &= I^{(0)} + \varepsilon I^{(1)} + \varepsilon^2 I^{(2)} + \cdots, \\ T &= T^{(0)} + \varepsilon T^{(1)} + \varepsilon^2 T^{(2)} + \cdots. \end{aligned} \tag{2.3}$$

By substituting ansatz (2.3) into equation (2.2a) and collecting the terms of the same order in ε, we have

$$\mathcal{O}\left(\frac{1}{\varepsilon^2}\right): I^{(0)} = J^{(0)}, \tag{2.4a}$$

$$\mathcal{O}\left(\frac{1}{\varepsilon}\right): c\boldsymbol{n}\cdot\nabla I^{(0)} = c\sigma_s\left(J^{(1)} - I^{(1)}\right) + \boldsymbol{n}\cdot\boldsymbol{v}\sigma_s\left(I^{(0)} + 3J^{(0)}\right). \tag{2.4b}$$

Multiplying both sides of (2.2a) by $\boldsymbol{n}$, taking its integral with respect to $\boldsymbol{n}$ and combining the obtained equation with (2.2c), one can get the following momentum conservation equation:

$$\partial_t\left(\frac{\rho\boldsymbol{v}}{\mathcal{P}_0} + \frac{4\pi\varepsilon}{c}\langle\boldsymbol{n}I\rangle\right) + \nabla\cdot\left(\frac{\rho\boldsymbol{v}\boldsymbol{v} - \boldsymbol{B}\boldsymbol{B} + P^*}{\mathcal{P}_0} + 4\pi\langle\boldsymbol{n}^2 I\rangle\right) = 0. \tag{2.5}$$

By using (2.4a) and $\langle\boldsymbol{n}^2\rangle = \frac{1}{3}$, when $\varepsilon \to 0$, (2.5) gives

$$\partial_t(\rho^{(0)}\boldsymbol{v}^{(0)}) + \nabla\cdot\left(\rho^{(0)}\boldsymbol{v}^{(0)}\boldsymbol{v}^{(0)} - \boldsymbol{B}^{(0)}\boldsymbol{B}^{(0)} + (P^*)^{(0)}\right) = -\frac{4\pi\mathcal{P}_0}{3}\nabla J^{(0)}. \tag{2.6}$$

By taking the integral with respect to $\boldsymbol{n}$ on both sides of (2.2a), and combining it with (2.2d), one can obtain the energy conservation equation

$$\partial_t\left(\frac{E}{\mathcal{P}_0} + 4\pi\langle I\rangle\right) + \nabla\cdot\left[\frac{(E+P^*)\boldsymbol{v} - \boldsymbol{B}(\boldsymbol{B}\cdot\boldsymbol{v})}{\mathcal{P}_0} + \frac{4\pi c\langle\boldsymbol{n}I\rangle}{\varepsilon}\right] = 0. \tag{2.7}$$

By using (2.4a), when $\varepsilon \to 0$, (2.7) gives

$$\partial_t\left(\frac{E^{(0)}}{\mathcal{P}_0}+4\pi\left\langle I^{(0)}\right\rangle\right)+\nabla\cdot\left[\frac{(E^{(0)}+(P^*)^{(0)})\boldsymbol{v}^{(0)}-\boldsymbol{B}^{(0)}(\boldsymbol{B}^{(0)}\cdot\boldsymbol{v}^{(0)})}{\mathcal{P}_0}+4\pi c\left\langle \boldsymbol{n}I^{(1)}\right\rangle\right]=0.$$

Noting (2.4b), we find

$$\partial_t\left(E^{(0)}+4\pi\mathcal{P}_0J^{(0)}\right)+\nabla\cdot\left[(E^{(0)}+(P^*)^{(0)})\boldsymbol{v}^{(0)}-\boldsymbol{B}^{(0)}(\boldsymbol{B}^{(0)}\cdot\boldsymbol{v}^{(0)})+\frac{16\pi\mathcal{P}_0}{3}\boldsymbol{v}^{(0)}J^{(0)}-\frac{4\pi c\mathcal{P}_0}{3\sigma_s}\nabla J^{(0)}\right]=0. \tag{2.8}$$

(2.2b), (2.6), (2.8) and (2.2e) give four equations for $\rho,\ \rho\boldsymbol{v},\ E,\ J,\ \boldsymbol{B}$, to obtain a closed system, we need one more equation for J. Taking $\langle\cdot\rangle$ on both sides of equation (2.2a), yields:

$$\partial_t\langle I\rangle+\frac{c}{\varepsilon}\nabla\cdot\langle\boldsymbol{n}I\rangle=\frac{c}{4\pi\varepsilon}S_{re}.$$

By using the expansion in (2.3) and (2.4a), the leading order terms are

$$4\pi\partial_t\left\langle I^{(0)}\right\rangle+4\pi c\nabla\cdot\left\langle\boldsymbol{n}I^{(1)}\right\rangle=c\sigma_a\left((T^{(0)})^4-4\pi\left\langle I^{(0)}\right\rangle\right)-4\pi\sigma_s\frac{\boldsymbol{v}^{(0)}}{c}\left[c\left\langle\boldsymbol{n}I^{(1)}\right\rangle-\boldsymbol{v}^{(0)}\left(\left\langle I^{(0)}\right\rangle+\left\langle\boldsymbol{n}^2I^{(0)}\right\rangle\right)\right],$$

then from (2.4b), one gets

$$4\pi\partial_tJ^{(0)}+\nabla\cdot\left(\frac{16\pi}{3}\boldsymbol{v}^{(0)}J^{(0)}-\frac{4\pi c}{3\sigma_s}\nabla J^{(0)}\right)=c\sigma_a\left((T^{(0)})^4-4\pi J^{(0)}\right)+\frac{4\pi}{3}\boldsymbol{v}^{(0)}\nabla J^{(0)}. \tag{2.9}$$

Therefore, when $\varepsilon\to 0$ in (2.2), the solution can be approximated by the solution of the following non-equilibrium system:

$$\begin{cases}\partial_t\rho+\nabla\cdot(\rho\boldsymbol{v})=0, & (2.10a)\\ \partial_t(\rho\boldsymbol{v})+\nabla\cdot(\rho\boldsymbol{v}\boldsymbol{v}-\boldsymbol{B}\boldsymbol{B}+P^*)=-\dfrac{4\pi\mathcal{P}_0}{3}\nabla J, & (2.10b)\\ \partial_t\left(E+4\pi\mathcal{P}_0J\right)+\nabla\cdot\left[(E+P^*)\boldsymbol{v}-\boldsymbol{B}(\boldsymbol{B}\cdot\boldsymbol{v})+\dfrac{16\pi\mathcal{P}_0}{3}\boldsymbol{v}J\right]=\nabla\cdot\left(\dfrac{4\pi c\mathcal{P}_0}{3\sigma_s}\nabla J\right), & (2.10c)\\ 4\pi\partial_tJ+\nabla\cdot\left(\dfrac{16\pi}{3}\boldsymbol{v}J-\dfrac{4\pi c}{3\sigma_s}\nabla J\right)=c\sigma_a\left(T^4-4\pi J\right)+\dfrac{4\pi}{3}\boldsymbol{v}\nabla J, & (2.10d)\\ \partial_t\boldsymbol{B}+\nabla\times(\boldsymbol{v}\times\boldsymbol{B})=0. & (2.10e)\end{cases}$$

Here, the non-equilibrium system indicates that J is away from $\frac{T^4}{4\pi}$, while we will see in section 2.2 that the equilibrium diffusion limit indicates that $J\approx\frac{T^4}{4\pi}$.

2.2. **The equilibrium diffusion limit.** The setting of $\mathcal{P}_0$ and $\mathcal{C}$ in this regime are the same with the non-equilibrium regime. Moreover, we assume $\mathscr{L}_a=1/\varepsilon,\mathscr{L}_s=\varepsilon$, and the radiation intensity I adapt to the material temperature. In summary, we consider the following scaling

$$\mathscr{L}_a=1/\varepsilon,\quad \mathscr{L}_s=\varepsilon,\quad \mathcal{P}_0=\mathcal{O}(1),\quad \mathcal{C}=c/\varepsilon.$$

This is called the equilibrium diffusion regime, which will give the classical equilibrium diffusion limit [19, 23, 25]. The RMHD system (2.1) becomes (after dropping the hat):

$$
\begin{cases}
\dfrac{\partial I}{\partial t} + \dfrac{c}{\varepsilon}\boldsymbol{n}\cdot\nabla I = \dfrac{c\sigma_a}{\varepsilon^2}\left(\dfrac{T^4}{4\pi} - I\right) + c\sigma_s(J-I) + 3\boldsymbol{n}\cdot\boldsymbol{v}\dfrac{\sigma_a}{\varepsilon}\left(\dfrac{T^4}{4\pi} - J\right) + \boldsymbol{n}\cdot\boldsymbol{v}\left(\dfrac{\sigma_a}{\varepsilon} + \varepsilon\sigma_s\right)(I+3J) \\
\qquad\qquad -2\varepsilon\sigma_s\boldsymbol{v}\cdot\boldsymbol{H} - (\sigma_a - \varepsilon^2\sigma_s)\dfrac{\boldsymbol{v}\cdot\boldsymbol{v}}{c}J - (\sigma_a - \varepsilon^2\sigma_s)\dfrac{\boldsymbol{v}\cdot(\boldsymbol{v}\cdot K)}{c}, & (2.11a) \\
\dfrac{\partial\rho}{\partial t} + \nabla\cdot(\rho\boldsymbol{v}) = 0, & (2.11b) \\
\dfrac{\partial(\rho\boldsymbol{v})}{\partial t} + \nabla\cdot(\rho\boldsymbol{v}\boldsymbol{v} - \boldsymbol{B}\boldsymbol{B} + P^*) = -\mathcal{P}_0\boldsymbol{S_{rp}}, & (2.11c) \\
\dfrac{\partial E}{\partial t} + \nabla\cdot[(E+P^*)\boldsymbol{v} - \boldsymbol{B}(\boldsymbol{B}\cdot\boldsymbol{v})] = -\dfrac{c}{\varepsilon}\mathcal{P}_0 S_{re}, & (2.11d) \\
\dfrac{\partial\boldsymbol{B}}{\partial t} + \nabla\times(\boldsymbol{v}\times\boldsymbol{B}) = 0\,, & (2.11e)
\end{cases}
$$

where

$$
S_{re} = \frac{\sigma_a}{\varepsilon}\left(T^4 - \frac{4\pi}{|V|}\int_V I\mathrm{d}\boldsymbol{n}\right) + (\varepsilon\sigma_a - \varepsilon^3\sigma_s)\frac{4\pi\boldsymbol{v}}{c^2|V|}\cdot\left[\frac{c}{\varepsilon}\int_V \boldsymbol{n}I\mathrm{d}\boldsymbol{n} - \left(\boldsymbol{v}\int_V I\mathrm{d}\boldsymbol{n} + \boldsymbol{v}\int_V \boldsymbol{n}^2 I\mathrm{d}\boldsymbol{n}\right)\right],
$$

$$
\boldsymbol{S_{rp}} = -\frac{4\pi(\varepsilon^2\sigma_s + \sigma_a)}{c|V|}\left[\frac{c}{\varepsilon}\int_V \boldsymbol{n}I\mathrm{d}\boldsymbol{n} - \left(\boldsymbol{v}\int_V I\mathrm{d}\boldsymbol{n} + \boldsymbol{v}\int_V \boldsymbol{n}^2 I\mathrm{d}\boldsymbol{n}\right)\right] + \frac{\boldsymbol{v}}{c}\sigma_a\left(T^4 - \frac{4\pi}{|V|}\int_V I\mathrm{d}\boldsymbol{n}\right).
$$

Using the same expansion as in (2.3), one has

$$
\begin{aligned}
T^4 &= (T^{(0)} + \varepsilon T^{(1)} + \varepsilon^2 T^{(2)} + \cdots)^4 \\
&= (T^{(0)})^4 + 4\varepsilon(T^{(0)})^3 T^{(1)} + \cdots.
\end{aligned} \tag{2.12}
$$

Then substituting (2.12) into (2.11a) and collecting the terms of the same order of ε, one gets

$$
\mathcal{O}\left(\frac{1}{\varepsilon^2}\right): I^{(0)} = \frac{(T^{(0)})^4}{4\pi}, \tag{2.13a}
$$

$$
\mathcal{O}\left(\frac{1}{\varepsilon}\right): c\boldsymbol{n}\cdot\nabla I^{(0)} = c\sigma_a\left(\frac{4(T^{(0)})^3 T^{(1)}}{4\pi} - I^{(1)}\right) + \boldsymbol{n}\cdot\boldsymbol{v}\sigma_a\left(I^{(0)} + \frac{3(T^{(0)})^4}{4\pi}\right), \tag{2.13b}
$$

by similar calculations in section 2.1, one can get the following equilibrium diffusion limit:

$$
\begin{cases}
\partial_t\rho + \nabla\cdot(\rho\boldsymbol{v}) = 0, & (2.14a) \\
\partial_t(\rho\boldsymbol{v}) + \nabla\cdot(\rho\boldsymbol{v}\boldsymbol{v} - \boldsymbol{B}\boldsymbol{B} + P^*) = -\dfrac{\mathcal{P}_0}{3}\nabla T^4, & (2.14b) \\
\partial_t\left(E + \mathcal{P}_0 T^4\right) + \nabla\cdot\left[(E+P^*)\boldsymbol{v} - \boldsymbol{B}(\boldsymbol{B}\cdot\boldsymbol{v}) + \dfrac{4\mathcal{P}_0}{3}\boldsymbol{v}T^4\right] = \nabla\cdot\left(\dfrac{c\mathcal{P}_0}{3\sigma_a}\nabla T^4\right), & (2.14c) \\
\partial_t\boldsymbol{B} + \nabla\times(\boldsymbol{v}\times\boldsymbol{B}) = 0. & (2.14d)
\end{cases}
$$

As we can see, when $J = \frac{T^4}{4\pi}$ in (2.10), the non-equilibrium diffusion system (2.10) is the same as the equilibrium diffusion system (2.14), which indicates J is close to $\frac{T^4}{4\pi}$ in the equilibrium system (2.11).

3. Time discretization for the RMHD

In this section, based on a decomposition for radiation intensity I, we will present a semi-discretization for the RMHD and show its AP property for any dimensions in space and angular variables.

3.1. **A decomposition.** To preserve the asymptotic limit of (2.1) while keeping the computational complexity under control, the intensity I will be decomposed into three parts, and each of them is treated in a different way. More precisely, we decompose $I(t,x,n)$ as follows:

$$I(t,x,\boldsymbol{n}) = \langle I\rangle + 3\boldsymbol{n}\langle \boldsymbol{n}I\rangle + \varepsilon Q(t,x,\boldsymbol{n}), \tag{3.1a}$$

$$:= J(t,x) + \varepsilon \boldsymbol{n}R(t,x) + \varepsilon Q(t,x,\boldsymbol{n}), \tag{3.1b}$$

with $3\langle \boldsymbol{n}I\rangle = \varepsilon R$. Then taking $\langle \boldsymbol{n}\cdot\rangle$ on both sides of (3.1a) and using the condition $\langle \boldsymbol{n}^2\rangle = \frac{1}{3}$ yields

$$\langle \boldsymbol{n}I\rangle = \langle \boldsymbol{n}I\rangle + \varepsilon\langle \boldsymbol{n}Q\rangle,$$

which gives

$$\langle \boldsymbol{n}Q\rangle = 0. \tag{3.2}$$

Moreover, taking $\langle\cdot\rangle$ on (3.1b), yields

$$\langle I\rangle = \langle J + \varepsilon\boldsymbol{n}R + \varepsilon Q\rangle = \langle J + \varepsilon Q\rangle = \langle I\rangle + \varepsilon\langle Q\rangle,$$

which implies

$$\langle Q\rangle = 0. \tag{3.3}$$

Substituting the decomposition (3.1) into system (2.2) leads to

$$\begin{cases}
\partial_t\left(J + \varepsilon\left(\boldsymbol{n}R + Q\right)\right) + \dfrac{c}{\varepsilon}\boldsymbol{n}\nabla\cdot\left(J + \varepsilon\left(\boldsymbol{n}R + Q\right)\right) = c\sigma_a\left(\dfrac{T^4}{4\pi} - J\right) - \left(c\varepsilon\sigma_a + \dfrac{c\sigma_s}{\varepsilon}\right)(\boldsymbol{n}R + Q) \\
-\dfrac{2}{3}\sigma_s\boldsymbol{v}R + \boldsymbol{n}\boldsymbol{v}\left(\varepsilon\sigma_a + \dfrac{\sigma_s}{\varepsilon}\right)\left(4J + \varepsilon(\boldsymbol{n}R + Q)\right) + 3\varepsilon\sigma_a\boldsymbol{n}\boldsymbol{v}\left(\dfrac{T^4}{4\pi} - J\right) - \dfrac{(\varepsilon^2\sigma_a - \sigma_s)\boldsymbol{v}\cdot\boldsymbol{v}}{c}\left(\dfrac{4}{3}J + \varepsilon K_Q\right), & (3.4a) \\
\dfrac{\partial\rho}{\partial t} + \nabla\cdot(\rho\boldsymbol{v}) = 0, & (3.4b) \\
\dfrac{\partial(\rho\boldsymbol{v})}{\partial t} + \nabla\cdot(\rho\boldsymbol{v}\boldsymbol{v} - \boldsymbol{B}\boldsymbol{B} + P^*) = -\mathcal{P}_0\widehat{\boldsymbol{S_{rp}}}, & (3.4c) \\
\dfrac{\partial E}{\partial t} + \nabla\cdot[(E + P^*)\boldsymbol{v} - \boldsymbol{B}(\boldsymbol{B}\cdot\boldsymbol{v})] = -\dfrac{c}{\varepsilon}\mathcal{P}_0\widehat{S_{re}}, & (3.4d) \\
\dfrac{\partial\boldsymbol{B}}{\partial t} + \nabla\times(\boldsymbol{v}\times\boldsymbol{B}) = 0, & (3.4e)
\end{cases}$$

where $K_Q = \langle \boldsymbol{n}^2 Q\rangle$ and

$$\widehat{S_{re}} = \varepsilon\sigma_a(T^4 - 4\pi J) + 4\pi(\varepsilon^3\sigma_a - \varepsilon\sigma_s)\frac{\boldsymbol{v}}{c^2}\cdot\left[\frac{c}{3}R - \boldsymbol{v}\left(\frac{4}{3}J + \varepsilon K_Q\right)\right],$$

$$\widehat{\boldsymbol{S_{rp}}} = -\frac{4\pi(\sigma_s + \varepsilon^2\sigma_a)}{c}\left[\frac{c}{3}R - \boldsymbol{v}\left(\frac{4}{3}J + \varepsilon K_Q\right)\right] - \frac{\varepsilon^2\boldsymbol{v}}{c}\sigma_a(T^4 - 4\pi J).$$

(3.4a) has three unknown functions, J, R and Q. Thanks to the properties of Q in (3.2),(3.3), the zeroth and first moment equations of (3.4a) have no time derivatives with respect to Q. Therefore, instead of solving the RMHD system (3.4) directly, we take the zeroth and first moments of (3.4a), and then couple them together with (3.4b)–(3.4e) to solve variables $\rho, J, R, \boldsymbol{v}, T, \boldsymbol{B}$. More precisely, we have

$$\begin{cases}
\partial_t J + \dfrac{c}{3}\nabla\cdot R = \dfrac{c}{4\pi\varepsilon}\widehat{S_{re}}, \\
\dfrac{\varepsilon}{3}\partial_t R + \dfrac{c}{3\varepsilon}\nabla\cdot J + c\nabla\cdot K_Q = \dfrac{c}{4\pi\varepsilon}\widehat{\boldsymbol{S_{rp}}},
\end{cases} \tag{3.5}$$

coupled with (3.4b)–(3.4e) and by treating K_Q explicitly, one can update the macroscopic quantities first. Then Q can be updated implicitly by the first equation in system (3.4a), and the new I can be given by (3.1). The details are illustrated in the next two subsections.

3.2. **The time discretization for the non-equilibrium regime.** Let

$$t^s = s\Delta t, \qquad s = 0, 1, 2, \cdots,$$

and

$$I^s \approx I(x, t^s, n), \qquad \rho^s \approx \rho(x, t^s, n), \qquad \boldsymbol{v}^s \approx \boldsymbol{v}(x, t^s, n),$$

$$T^s \approx T(x, t^s, n), \qquad \boldsymbol{B}^s \approx \boldsymbol{B}(x, t^s, n).$$

We use the following semi-discrete scheme in time for (3.4), which reads:

$$\begin{cases} \dfrac{J^{s+1}-J^s}{\Delta t} + \varepsilon \boldsymbol{n}\dfrac{R^{s+1}-R^s}{\Delta t} + \varepsilon\dfrac{Q^{s+1}-Q^s}{\Delta t} + \dfrac{c}{\varepsilon}\boldsymbol{n}\nabla\cdot J^{s+1} + c\boldsymbol{n}\nabla\cdot(\boldsymbol{n}R^{s+1}+Q^s) \\ \qquad = c\sigma_a\left(\dfrac{(T^{s+1})^4}{4\pi} - J^{s+1}\right) - \left(c\varepsilon\sigma_a + \dfrac{c\sigma_s}{\varepsilon}\right)(\boldsymbol{n}R^{s+1}+Q^{s+1}) - \dfrac{2}{3}\sigma_s\boldsymbol{v}^{s+1}R^{s+1} \\ \qquad +3\varepsilon\sigma_a\boldsymbol{n}\boldsymbol{v}^{s+1}\left(\dfrac{(T^{s+1})^4}{4\pi} - J^{s+1}\right) + \boldsymbol{n}\boldsymbol{v}^{s+1}\left(\varepsilon\sigma_a + \dfrac{\sigma_s}{\varepsilon}\right)(4J^{s+1} + \varepsilon(\boldsymbol{n}R^{s+1}+Q^s)) \\ \qquad\qquad -(\varepsilon^2\sigma_a - \sigma_s)\dfrac{\boldsymbol{v}^{s+1}\cdot\boldsymbol{v}^{s+1}}{c}\left(\dfrac{4}{3}J^{s+1} + \varepsilon K_Q^s\right), & (3.6a) \\ \dfrac{\rho^{s+1}-\rho^s}{\Delta t} + \nabla\cdot(\rho^s\boldsymbol{v}^s) = 0, & (3.6b) \\ \dfrac{(\rho\boldsymbol{v})^{s+1}-(\rho\boldsymbol{v})^s}{\Delta t} + \nabla\cdot(\rho^s\boldsymbol{v}^s\boldsymbol{v}^s - \boldsymbol{B}^s\boldsymbol{B}^s + (P^s)^*) = -\mathcal{P}_0(\widehat{\boldsymbol{S_{rp}}})^{s+1}, & (3.6c) \\ a\dfrac{(\rho T)^{s+1}-(\rho T)^s}{\Delta t} + \dfrac{\rho^{s+1}(v^{s+1})^2 - \rho^s(v^s)^2}{2\Delta t} + \dfrac{(B^{s+1})^2-(B^s)^2}{2\Delta t} \\ \qquad\qquad +\nabla\cdot[(E^s + (P^*)^s)\boldsymbol{v}^s - \boldsymbol{B}^s(\boldsymbol{B}^s\cdot\boldsymbol{v}^s)] = -\dfrac{c}{\varepsilon}\mathcal{P}_0(\widehat{S_{re}})^{s+1}, & (3.6d) \\ \dfrac{\boldsymbol{B}^{s+1}-\boldsymbol{B}^s}{\Delta t} + \nabla\times(\boldsymbol{v}^s\times\boldsymbol{B}^s) = 0. & (3.6e) \end{cases}$$

where $K_Q^s = \left\langle \boldsymbol{n}^2 Q^s \right\rangle$ and

$$(\widehat{S_{re}})^{s+1} = \varepsilon\sigma_a((T^{s+1})^4 - 4\pi J^{s+1}) + 4\pi(\varepsilon^3\sigma_a - \varepsilon\sigma_s)\frac{\boldsymbol{v}^{s+1}}{c^2}\left[\frac{c}{3}R^{s+1} - \boldsymbol{v}^{s+1}\left(\frac{4}{3}J^{s+1} + \varepsilon K_Q^s\right)\right],$$

$$(\widehat{\boldsymbol{S_{rp}}})^{s+1} = -\frac{4\pi(\sigma_s + \varepsilon^2\sigma_a)}{c}\left[\frac{c}{3}R^{s+1} - \boldsymbol{v}^{s+1}\left(\frac{4}{3}J^{s+1} + \varepsilon K_Q^s\right)\right] - \frac{\varepsilon^2\boldsymbol{v}^{s+1}}{c}\sigma_a((T^{s+1})^4 - 4\pi J^{s+1}).$$

The zeroth and first moment equations of (3.6a) are

$$\begin{cases} \dfrac{J^{s+1}-J^s}{\Delta t} + \dfrac{c}{3}\nabla\cdot R^{s+1} = \dfrac{c}{4\pi\varepsilon}(\widehat{S_{re}})^{s+1}, & (3.7a) \\ \dfrac{\varepsilon^2}{3c}\dfrac{R^{s+1}-R^s}{\Delta t} + \dfrac{1}{3}\nabla\cdot J^{s+1} + \varepsilon\nabla\cdot K_Q^s = \dfrac{(\widehat{\boldsymbol{S_{rp}}})^{s+1}}{4\pi}. & (3.7b) \end{cases}$$

We first update $\rho, \boldsymbol{B}$ by (3.6b), (3.6e) and then solve (3.6c), (3.6d) and (3.7) to get $J, R, \boldsymbol{v}, T$. Q^{s+1} can then be updated implicitly by equation (3.6a), and we get the I^{s+1} by using (3.1).

The diffusion limit of (3.7): Then we will show the AP property of the semi-discretization (3.7). From (3.7b),

$$R^{s+1} = \frac{4\boldsymbol{v}^{s+1}J^{s+1}}{c} - \frac{\nabla\cdot J^{s+1}}{\sigma_s} + \mathcal{O}(\varepsilon)\,. \tag{3.8}$$

Multiplying equation (3.7a) by $4\pi\mathcal{P}_0$, and adding it up with equation (3.6d), the terms on the right hand sides cancel. By using (3.8), and sending $\varepsilon \to 0$ in $4\pi\mathcal{P}_0 \times$ (3.7a) + (3.6d) yields

$$\begin{aligned} a\frac{(\rho T)^{s+1}-(\rho T)^s}{\Delta t} + \frac{\rho^{s+1}(v^{s+1})^2-\rho^s(v^s)^2}{2\Delta t} + \frac{(B^{s+1})^2-(B^s)^2}{2\Delta t} + 4\pi\mathcal{P}_0\frac{J^{s+1}-J^s}{\Delta t} \\ +\nabla\cdot\left[(E^s+(P^s)^*)\boldsymbol{v}^s - \boldsymbol{B}^s(\boldsymbol{B}^s\cdot\boldsymbol{v}^s) + \frac{16\pi\mathcal{P}_0}{3}\boldsymbol{v}^{s+1}J^{s+1}\right] = \nabla\cdot\left(\frac{4\pi c\mathcal{P}_0}{3\sigma_s}\nabla J^{s+1}\right). \end{aligned} \tag{3.9}$$

This is a semi-discretization for (2.10c). Then multiplying equation (3.7b) by $4\pi\mathcal{P}_0$, and adding it to equation (3.6c), sending $\varepsilon \to 0$, formally one gets

$$\frac{(\rho\boldsymbol{v})^{s+1}-(\rho\boldsymbol{v})^s}{\Delta t} + \nabla\cdot(\rho^s\boldsymbol{v}^s\boldsymbol{v}^s - \boldsymbol{B}^s\boldsymbol{B}^s + (P^*)^s) = -\frac{4\pi\mathcal{P}_0}{3}\nabla\cdot J^{s+1}. \tag{3.10}$$

This is a semi-discretization for (2.10b). Sending $\varepsilon \to 0$ in equation (3.7a), yields

$$4\pi\frac{J^{s+1}-J^s}{\Delta t} + \frac{4\pi c}{3}\nabla\cdot R^{s+1} = c\sigma_a((T^{s+1})^4 - 4\pi J^{s+1}) - 4\pi\sigma_s\frac{\boldsymbol{v}^{s+1}}{c}\left(\frac{c}{3}R^{s+1} - \frac{4}{3}\boldsymbol{v}^{s+1}J^{s+1}\right), \tag{3.11}$$

using (3.8) in (3.11), we get

$$4\pi\frac{J^{s+1}-J^s}{\Delta t} + \frac{16\pi}{3}\nabla\cdot(\boldsymbol{v}^{s+1}J^{s+1}) - \nabla\cdot\left(\frac{4\pi c}{3\sigma_s}\nabla J^{s+1}\right) = c\sigma_a((T^{s+1})^4 - 4\pi J^{s+1}) + \frac{4\pi}{3}\boldsymbol{v}^{s+1}\nabla\cdot J^{s+1}, \tag{3.12}$$

which is a semi-discretization (2.10d).

3.3. **The time discretization for the equilibrium regime.** We substitute the decomposition in (3.1) into the RMHD system (2.11), and the time discretization of (2.11) is same with (3.6) except the RTE and source terms $(\widehat{S_{re}})^{s+1}$ and $(\widehat{\boldsymbol{S_{rp}}})^{s+1}$, which read:

$$\begin{aligned} \frac{J^{s+1}-J^s}{\Delta t} + \varepsilon\boldsymbol{n}\frac{R^{s+1}-R^s}{\Delta t} + \varepsilon\frac{Q^{s+1}-Q^s}{\Delta t} + \frac{c}{\varepsilon}\boldsymbol{n}\nabla\cdot J^{s+1} + c\boldsymbol{n}\nabla\cdot(\boldsymbol{n}R^{s+1}+Q^s) = \frac{c\sigma_a}{\varepsilon^2}\left(\frac{(T^{s+1})^4}{4\pi} - J^{s+1}\right) \\ -\left(\frac{c\sigma_a}{\varepsilon} + c\varepsilon\sigma_s\right)(\boldsymbol{n}R^{s+1}+Q^{s+1}) - \frac{2}{3}\varepsilon^2\sigma_s\boldsymbol{v}^{s+1}R^{s+1} - (\sigma_a - \varepsilon^2\sigma_s)\frac{\boldsymbol{v}^{s+1}\cdot\boldsymbol{v}^{s+1}}{c}\left(\frac{4}{3}J^{s+1} + \varepsilon K_Q^s\right) \\ +3\frac{\sigma_a}{\varepsilon}\boldsymbol{n}\boldsymbol{v}^{s+1}\left(\frac{(T^{s+1})^4}{4\pi} - J^{s+1}\right) + \boldsymbol{n}\boldsymbol{v}^{s+1}\left(\frac{\sigma_a}{\varepsilon} + \varepsilon\sigma_s\right)(4J^{s+1} + \varepsilon(\boldsymbol{n}R^{s+1}+Q^s)), \end{aligned} \tag{3.13}$$

and

$$(\widehat{S_{re}})^{s+1} = \frac{\sigma_a}{\varepsilon}((T^{s+1})^4 - 4\pi J^{s+1}) + 4\pi(\varepsilon\sigma_a - \varepsilon^3\sigma_s)\frac{\boldsymbol{v}^{s+1}}{c^2}\left[\frac{c}{3}R^{s+1} - \boldsymbol{v}^{s+1}\left(\frac{4}{3}J^{s+1} + \varepsilon K_Q^s\right)\right], \tag{3.14}$$

$$(\widehat{\boldsymbol{S_{rp}}})^{s+1} = -\frac{4\pi(\varepsilon^2\sigma_s + \sigma_a)}{c}\left[\frac{c}{3}R^{s+1} - \boldsymbol{v}^{s+1}\left(\frac{4}{3}J^{s+1} + \varepsilon K_Q^s\right)\right] - \frac{\boldsymbol{v}^{s+1}}{c}\sigma_a((T^{s+1})^4 - 4\pi J^{s+1}). \tag{3.15}$$

Moreover, the procedure of solving the equilibrium case is the same as for (3.6).

The diffusion limit of the equilibrium regime: The derivation of the equilibrium diffusion limit is similar to the non-equilibrium case, but requires additional analysis for the zeroth moment of equation (3.13). Sending $\varepsilon \to 0$ in the zeroth moment equation of (3.13), one gets

$$\sigma_a((T^{s+1})^4 - 4\pi J^{s+1}) + \mathcal{O}(\varepsilon^2) = 0,$$

which implies

$$4\pi J^{s+1} = (T^{s+1})^4 + \mathcal{O}(\varepsilon^2).$$

Therefore, (3.9) and (3.10) in the equilibrium regime become

$$
\begin{aligned}
a\frac{(\rho T)^{s+1}-(\rho T)^s}{\Delta t}+\frac{\rho^{s+1}(v^{s+1})^2-\rho^s(v^s)^2}{2\Delta t}+\frac{(B^{s+1})^2-(B^s)^2}{2\Delta t}+\mathcal{P}_0\frac{(T^{s+1})^4-(T^s)^4}{\Delta t}\\
+\nabla\cdot\left[(E^s+(P^s)^*)\boldsymbol{v}^s-\boldsymbol{B}^s(\boldsymbol{B}^s\cdot\boldsymbol{v}^s)+\frac{4\mathcal{P}_0}{3}\boldsymbol{v}^{s+1}(T^{s+1})^4\right]=\nabla\cdot\left(\frac{4\pi c\mathcal{P}_0}{3\sigma_a}\nabla(T^{s+1})^4\right),\\
\frac{(\rho\boldsymbol{v})^{s+1}-(\rho\boldsymbol{v})^s}{\Delta t}+\nabla\cdot(\rho^s\boldsymbol{v}^s\boldsymbol{v}^s-\boldsymbol{B}^s\boldsymbol{B}^s+(P^*)^s)=-\frac{\mathcal{P}_0}{3}\nabla\cdot(T^{s+1})^4,
\end{aligned}
$$

which gives a semi-discretization of system (2.14).

4. The full discretization for the non-equilibrium regime

For the ease of exposition, we will explain our spatial discretion in 1D. That is, $x\in[0,L]$, $n\in[-1,1]$, and $\langle f(n)\rangle=\frac{1}{2}\int_{-1}^1 f(n)\mathrm{d}n$. Recall the RMHD for the non-equilibrium case in the slab geometry:

$$
\begin{cases}
\partial_t I+\frac{c}{\varepsilon}n\partial_x I=c\sigma_a\left(\frac{T^4}{4\pi}-I\right)+\frac{c\sigma_s}{\varepsilon^2}(J-I)+3\varepsilon n v_x\sigma_a\left(\frac{T^4}{4\pi}-J\right)+nv_x\left(\varepsilon\sigma_a+\frac{\sigma_s}{\varepsilon}\right)(I+3J)\\
\qquad -2\frac{\sigma_s}{\varepsilon}v_x\cdot H-(\varepsilon^2\sigma_a-\sigma_s)\frac{v_x\cdot v_x}{c}J-(\varepsilon^2\sigma_a-\sigma_s)\frac{v_x\cdot(v_x\cdot K)}{c}, & (4.1a)\\
\partial_t\rho+\partial_x(\rho v_x)=0, & (4.1b)\\
\partial_t(\rho v_x)+\partial_x\left(\rho v_x^2+p+B^2/2+B_x^2\right)=-\mathcal{P}_0S_{rp}, & (4.1c)\\
\partial_t(\rho v_y)+\partial_x\left(\rho v_xv_y-B_xB_y\right)=0, & (4.1d)\\
\partial_t(\rho v_z)+\partial_x\left(\rho v_xv_z-B_xB_z\right)=0, & (4.1e)\\
\partial_t\left(a\rho T+\frac{\rho v^2+B^2}{2}\right)+\partial_x[(E+P^*)v_x-(\boldsymbol{B}\cdot\boldsymbol{v})B_x]=-\frac{c}{\varepsilon}\mathcal{P}_0S_{re}, & (4.1f)\\
\partial_t B_y+\partial_x(B_yv_x-B_xv_y)=0, & (4.1g)\\
\partial_t B_z+\partial_x(B_zv_x-B_xv_z)=0, & (4.1h)
\end{cases}
$$

where

$$
S_{re}=\varepsilon\sigma_a\left(T^4-2\pi\int_{-1}^1 I\mathrm{d}n\right)+2\pi(\varepsilon^3\sigma_a-\varepsilon\sigma_s)\frac{v_x}{c^2}\left[\frac{c}{\varepsilon}\int_{-1}^1 nI\mathrm{d}n-\left(v_x\int_{-1}^1 I\mathrm{d}n+v_x\int_{-1}^1 n^2I\mathrm{d}n\right)\right],
$$

$$
S_{rp}=-\frac{2\pi(\sigma_s+\varepsilon^2\sigma_a)}{c}\left[\frac{c}{\varepsilon}\int_{-1}^1 nI\mathrm{d}n-\left(v_x\int_{-1}^1 I\mathrm{d}n+v_x\int_{-1}^1 n^2I\mathrm{d}n\right)\right]+\frac{v_x}{c}\varepsilon^2\sigma_a\left(T^4-2\pi\int_{-1}^1 I\mathrm{d}n\right),
$$

and v_x, v_y and v_z are fluid velocity in the $x-$, $y-$, and $z-$directions, respectively. B_x, B_y and B_z are magnetic flux in the $x-$, $y-$, and $z-$directions, respectively. The boundary condition becomes

$$
I(t,0,n)=b_{\mathrm{L}}(t,n),\quad\text{for}\quad n>0;\qquad I(t,L,n)=b_{\mathrm{R}}(t,n),\quad\text{for}\quad n<0. \tag{4.2}
$$

Higher dimensions can be treated in the dimension by dimension manner. Let $[a,b]$ be the computational domain, $\Delta x=(b-a)/N_x$, and we consider the uniform mesh as follows

$$
x_{i-\frac{1}{2}}=a+(i-1)\Delta x,\quad i=1,2\cdots,N_x+1,
$$

and let

$$
\begin{aligned}
x_{\frac{1}{2}}=a<x_1<x_{\frac{3}{2}}<\cdots<x_{i-\frac{1}{2}}<x_i<x_{i+\frac{1}{2}}<\cdots<x_{N_x}<x_{N_x+\frac{1}{2}}=b,\\
x_i=\left(x_{i-\frac{1}{2}}+x_{i+\frac{1}{2}}\right)/2,\qquad\text{for } i=1,\cdots,N_x.
\end{aligned}
$$

To get a consistent stencil in spatial discretization, we use the unified gas kinetic scheme (UGKS) for spatial discretization [22]. Other space discretization that is AP can be applied as well. The most crucial point is that the space discretization of the MHD system has to be consistent with that of RTE.

4.1. **A finite volume approach.** UGKS is a finite volume method, integrating RMHD system (4.1) over $[t_s, t_{s+1}]$ and $[x_{i-\frac{1}{2}}, x_{i+\frac{1}{2}}]$ gives

$$
\left\{
\begin{aligned}
&\frac{J_i^{s+1}-J_i^s}{\Delta t}+\varepsilon n\frac{R_i^{s+1}-R_i^s}{\Delta t}+\varepsilon\frac{Q_i^{s+1}-Q_i^s}{\Delta t}+\frac{1}{\Delta x}(\zeta_{i+\frac{1}{2}}-\zeta_{i-\frac{1}{2}})=\\
&\qquad\qquad c\sigma_a\left(\frac{(T_i^{s+1})^4}{4\pi}-J_i^{s+1}\right)-\left(c\varepsilon\sigma_a+\frac{c\sigma_s}{\varepsilon}\right)(nR_i^{s+1}+Q_i^{s+1})+G_i, &&(4.3a)\\
&\frac{\rho_i^{s+1}-\rho_i^s}{\Delta t}+\frac{1}{\Delta x}(F^s_{1,i+\frac{1}{2}}-F^s_{1,i-\frac{1}{2}})=0, &&(4.3b)\\
&\frac{(\rho v_x)_i^{s+1}-(\rho v_x)_i^s}{\Delta t}+\frac{1}{\Delta x}(F^s_{2,i+\frac{1}{2}}-F^s_{2,i-\frac{1}{2}})=-\mathcal{P}_0(\widehat{S_{rp}})_i^{s+1}, &&(4.3c)\\
&\frac{(\rho v_y)_i^{s+1}-(\rho v_y)_i^s}{\Delta t}+\frac{1}{\Delta x}(F^s_{3,i+\frac{1}{2}}-F^s_{3,i-\frac{1}{2}})=0, &&(4.3d)\\
&\frac{(\rho v_z)_i^{s+1}-(\rho v_z)_i^s}{\Delta t}+\frac{1}{\Delta x}(F^s_{4,i+\frac{1}{2}}-F^s_{4,i-\frac{1}{2}})=0, &&(4.3e)\\
&a\frac{(\rho T)_i^{s+1}-(\rho T)_i^s}{\Delta t}+\frac{(\rho v^2+B^2)_i^{s+1}-(\rho v^2+B^2)_i^s}{2\Delta t}+\frac{1}{\Delta x}(F^s_{5,i+\frac{1}{2}}-F^s_{5,i-\frac{1}{2}})=-\frac{c}{\varepsilon}\mathcal{P}_0(\widehat{S_{re}})_i^{s+1}, &&(4.3f)\\
&\frac{B_{y,i}^{s+1}-B_{y,i}^s}{\Delta t}+\frac{1}{\Delta x}(F^s_{6,i+\frac{1}{2}}-F^s_{6,i-\frac{1}{2}})=0, &&(4.3g)\\
&\frac{B_{z,i}^{s+1}-B_{z,i}^s}{\Delta t}+\frac{1}{\Delta x}(F^s_{7,i+\frac{1}{2}}-F^s_{7,i-\frac{1}{2}})=0, &&(4.3h)
\end{aligned}
\right.
$$

where G, $(\widehat{S_{re}})_i^{s+1}$ and $(\widehat{S_{rp}})_i^{s+1}$ are

$$
\begin{aligned}
G_i =&3\varepsilon\sigma_{a,i}nv_{x,i}^{s+1}\left(\frac{(T_i^{s+1})^4}{4\pi}-J_i^{s+1}\right)+nv_{x,i}^{s+1}\left(\varepsilon\sigma_{a,i}+\frac{\sigma_{s,i}}{\varepsilon}\right)\left(4J_i^{s+1}+\varepsilon(nR_i^{s+1}+Q_i^s)\right)\\
&-\frac{2}{3}\sigma_{s,i}v_{x,i}^{s+1}R_i^{s+1}-\frac{(\varepsilon^2\sigma_{a,i}-\sigma_{s,i})(v_{x,i}^{s+1})^2}{c}\left(\frac{4}{3}J_i^{s+1}+\varepsilon K_{Q,i}^s\right),
\end{aligned}
$$

$$
(\widehat{S_{re}})_i^{s+1}=4\pi\varepsilon\sigma_{a,i}\left(\frac{(T_i^{s+1})^4}{4\pi}-J_i^{s+1}\right)+\frac{4\pi(\varepsilon^3\sigma_{a,i}-\varepsilon\sigma_{s,i})v_{x,i}^{s+1}}{c^2}\left[\frac{c}{3}R_i^{s+1}-v_{x,i}^{s+1}\left(\frac{4}{3}J_i^{s+1}+\varepsilon K_{Q,i}^s\right)\right],
$$

$$
(\widehat{S_{rp}})_i^{s+1}=-\frac{4\pi(\sigma_{s,i}+\varepsilon^2\sigma_{a,i})}{c}\left[\frac{c}{3}R_i^{s+1}-v_{x,i}^{s+1}\left(\frac{4}{3}J_i^{s+1}+\varepsilon K_{Q,i}^s\right)\right]+\frac{4\pi\varepsilon^2\sigma_{a,i}v_{x,i}^{s+1}}{c}\left(\frac{(T_i^{s+1})^4}{4\pi}-J_i^{s+1}\right).
$$

Here the numerical fluxes $F^s_{\cdot,i\pm\frac{1}{2}}$ at the interfaces use Roe's Riemann solver [29], based on the piecewise linear reconstruction. At last, we discuss the microscopic flux ζ defined at the interface $x_{i+\frac{1}{2}}$ in (4.3a). In [22], all the terms of the microscopic flux are treated explicitly, in this paper all the terms except the initial value and K_Q are treated *implicitly*, and the processes of UGKS are detailed in Appendix A.

With the expressions (A.3), (A.4) and (A.6), the numerical flux $\zeta_{i+\frac{1}{2}}$ is

$$
\begin{aligned}
\zeta_{i+\frac{1}{2}}=&A_{i+\frac{1}{2}}n\left(I^{s,+}_{i+\frac{1}{2}}\mathbb{1}_{n>0}+I^{s,-}_{i+\frac{1}{2}}\mathbb{1}_{n<0}\right)+C^1_{i+\frac{1}{2}}nJ^{s+1}_{i+\frac{1}{2}}+\frac{C^2_{i+\frac{1}{2}}}{4\pi}n(T^{s+1}_{i+\frac{1}{2}})^4+F_{i+\frac{1}{2}}n\widehat{G}_{i+\frac{1}{2}}\\
&+D^1_{i+\frac{1}{2}}n^2\left(\delta_xJ^{s+1,+}_{i+\frac{1}{2}}\mathbb{1}_{n>0}+\delta_xJ^{s+1,-}_{i+\frac{1}{2}}\mathbb{1}_{n<0}\right)+\frac{D^2_{i+\frac{1}{2}}}{4\pi}n^2\left(\delta_x(T^{s+1,+}_{i+\frac{1}{2}})^4\mathbb{1}_{n>0}+\delta_x(T^{s+1,-}_{i+\frac{1}{2}})^4\mathbb{1}_{n<0}\right),
\end{aligned}
\tag{4.4}
$$

where $\mathbb{1}_{n\lesseqgtr 0}$ is the indicator function. Here the two approximations for I, from the left and from the right, at the interface $x_{i+\frac{1}{2}}$ are given by:

$$
I^{s,+}_{i+\frac{1}{2}}=I_i^s+\frac{\Delta x}{2}\delta_xI_i^s,\qquad I^{s,-}_{i+\frac{1}{2}}=I_{i+1}^s-\frac{\Delta x}{2}\delta_xI_{i+1}^s. \tag{4.5}
$$

Moreover, the coefficients in the numerical flux are given by:

$$
\begin{aligned}
&A = \frac{c}{\Delta t \varepsilon \mu}(1 - e^{-\mu \Delta t}),\\
&C^1 = \frac{c^2 \sigma_s}{\Delta t \varepsilon^3 \mu}\left(\Delta t - \frac{1}{\mu}(1 - e^{-\mu\Delta t})\right), \qquad C^2 = \frac{c^2\sigma_a}{\Delta t \varepsilon \mu}\left(\Delta t - \frac{1}{\mu}(1 - e^{-\mu\Delta t})\right),\\
&D^1 = -\frac{c^3\sigma_s}{\Delta t \varepsilon^4 \mu^2}\left(\Delta t\left(1 + e^{-\mu\Delta t}\right) - \frac{2}{\mu}\left(1 - e^{-\mu\Delta t}\right)\right),\\
&D^2 = -\frac{c^3\sigma_a}{\Delta t \varepsilon^2 \mu^2}\left(\Delta t\left(1 + e^{-\mu\Delta t}\right) - \frac{2}{\mu}\left(1 - e^{-\mu\Delta t}\right)\right),\\
&F = \frac{c}{\Delta t \varepsilon \mu}\left(\Delta t - \frac{1}{\mu}\left(1 - e^{-\mu\Delta t}\right)\right),
\end{aligned}
\tag{4.6}
$$

with $\mu = \frac{\varepsilon^2 c\sigma_a + c\sigma_s}{\varepsilon^2}$. For reader's convenience, the processes of UGKS are detailed in Appendix A.

To obtain a scheme that can update the quantities J,R, T and v_x, the zeroth moment and first moment of velocity field n for (4.3a) are needed. Integrating equation (4.3a) for n from -1 to 1, and multiplying the both sides by 4π, one can obtain

$$
4\pi\frac{J_i^{s+1} - J_i^s}{\Delta t} + \frac{2\pi}{\Delta x}\int_{-1}^{1} \widehat{\zeta}_{i+\frac12} - \widehat{\zeta}_{i-\frac12}\, dn = \frac{c}{\varepsilon}(\widehat{S_{re}})_i^{s+1},
\tag{4.7}
$$

where

$$
\begin{aligned}
\int_{-1}^{1}\widehat{\zeta}_{i+\frac12}\, dn =& \int_{-1}^{1} A_{i+\frac12} n\left(I^{s,+}_{i+\frac12}\mathbb{1}_{n>0} + I^{s,-}_{i+\frac12}\mathbb{1}_{n<0}\right) dn + \frac{2D^1_{i+\frac12}}{3}\frac{J_{i+1}^{s+1} - J_i^{s+1}}{\Delta x} + \frac{D^2_{i+\frac12}}{6\pi}\frac{(T_{i+1}^{s+1})^4 - (T_i^{s+1})^4}{\Delta x}\\
&+ F_{i+\frac12}\left[2\varepsilon\sigma_{a,i+\frac12} v^{s+1}_{x,i+\frac12}\left(\frac{(T^{s+1}_{i+\frac12})^4}{4\pi} - J^{s+1}_{i+\frac12}\right) + v^{s+1}_{x,i+\frac12}\frac{\sigma_{s,i+\frac12} + \varepsilon^2\sigma_{a,i+\frac12}}{\varepsilon}\left(\frac{8}{3}J^{s+1}_{i+\frac12} + 2\varepsilon K^s_{Q,i+\frac12}\right)\right].
\end{aligned}
$$

Multiplying equation (4.3a) by n, then integrating it for n from -1 to 1, and multiplying the both sides by 4π, one can obtain

$$
\frac{4\pi\varepsilon}{3}\frac{R_i^{s+1} - R_i^s}{\Delta t} + \frac{2\pi}{\Delta x}\int_{-1}^{1} n\left(\widehat{\zeta}_{i+\frac12} - \widehat{\zeta}_{i-\frac12}\right) dn = \frac{c}{\varepsilon}(\widehat{S_{rp}})_i^{s+1},
\tag{4.8}
$$

where

$$
\begin{aligned}
\int_{-1}^{1} n\widehat{\zeta}_{i+\frac12}\, dn =& \int_{-1}^{1} A_{i+\frac12} n^2\left(I^{s,+}_{i+\frac12}\mathbb{1}_{n>0} + I^{s,-}_{i+\frac12}\mathbb{1}_{n<0}\right) dn + \frac{C^1_{i+\frac12}}{3}(J_{i+1}^{s+1} + J_i^{s+1}) + \frac{C^2_{i+\frac12}}{12\pi}((T_{i+1}^{s+1})^4 + (T_i^{s+1})^4)\\
&+ F_{i+\frac12}\Bigg[v^{s+1}_{x,i+\frac12}\left(\varepsilon^2\sigma_{a,i+\frac12} + \sigma_{s,i+\frac12}\right)\left(\frac{2}{5}R^{s+1}_{i+\frac12} + \int_{-1}^{1} n^3 Q^s_{i+\frac12}\, dn\right) - \frac{4}{9}\sigma_{s,i+\frac12} v^{s+1}_{x,i+\frac12} R^{s+1}_{i+\frac12}\\
&- \frac{2(\varepsilon^2\sigma_{a,i+\frac12} - \sigma_{s,i+\frac12})(v^{s+1}_{x,i+\frac12})^2}{3c}\left(\frac{4}{3}J^{s+1}_{i+\frac12} + \varepsilon K^s_{Q,i+\frac12}\right)\Bigg].
\end{aligned}
$$

Coupling equations (4.7), (4.8), (4.3c) and (4.3f) as a system and solving the system, quantities J, T, R and v_x can be updated. Finally, quantity Q can be updated by equation (4.3a), and the new I can be given by using (3.1).

4.2. **The diffusion limit of** (4.3c)–(4.8)**.** Firstly, assuming σ_a and σ_s are positive, as $\varepsilon \to 0$, the leading order of the coefficients in the numerical flux (4.4) are

$$
\begin{aligned}
&A(\Delta t, \varepsilon, c, \sigma_a, \sigma_s) = 0 + \mathcal{O}(\varepsilon),\\
&\varepsilon C^1(\Delta t, \varepsilon, c, \sigma_a, \sigma_s) = c + \mathcal{O}(\varepsilon), \qquad \varepsilon C^2 = 0 + \mathcal{O}(\varepsilon),\\
&D^1 = -\frac{c}{\sigma_s} + \mathcal{O}(\varepsilon), \qquad D^2 = 0 + \mathcal{O}(\varepsilon),\\
&\frac{1}{\varepsilon}F = \frac{1}{\sigma_s} + \mathcal{O}(\varepsilon).
\end{aligned}
$$

This means the zero moment and the first moment of the numerical flux, as $\varepsilon \to 0$, have the following limit:

$$
\int_{-1}^{1} \widehat{\zeta}_{i+\frac{1}{2}} dn \to \frac{8}{3} v^{s+1}_{x,i+\frac{1}{2}} J^{s+1}_{i+\frac{1}{2}} - \frac{2c}{3\sigma_{s,i+\frac{1}{2}}} \frac{J^{s+1}_{i+1} - J^{s+1}_{i}}{\Delta x}, \tag{4.9}
$$

$$
\varepsilon \int_{-1}^{1} n\widehat{\zeta}_{i+\frac{1}{2}} dn \to \frac{c}{3}(J^{s+1}_{i+1} + J^{s+1}_{i}). \tag{4.10}
$$

Multiplying equation (4.7) by $\mathcal{P}_0$, and adding it up with equation (4.3f), the terms on the right hand sides cancel. By sending $\varepsilon \to 0$ and using (4.9) yields

$$
\begin{aligned}
a\frac{(\rho T)^{s+1}_i - (\rho T)^s_i}{\Delta t} &+ \frac{(\rho v^2 + B^2)^{s+1}_i - (\rho v^2 + B^2)^s_i}{2\Delta t} + 4\pi\mathcal{P}_0 \frac{J^{s+1}_i - J^s_i}{\Delta t} + \frac{1}{\Delta x}(F^s_{5,i+\frac{1}{2}} - F^s_{5,i-\frac{1}{2}})\\
&+ \frac{16\pi\mathcal{P}_0}{3} \frac{v^{s+1}_{x,i+\frac{1}{2}} J^{s+1}_{i+\frac{1}{2}} - v^{s+1}_{x,i-\frac{1}{2}} J^{s+1}_{i-\frac{1}{2}}}{\Delta x} = \frac{4\pi\mathcal{P}_0 c}{3\sigma_{s,i+\frac{1}{2}}\Delta x} \frac{J^{s+1}_{i+1} - J^{s+1}_{i}}{\Delta x} - \frac{4\pi\mathcal{P}_0 c}{3\sigma_{s,i-\frac{1}{2}}\Delta x} \frac{J^{s+1}_{i} - J^{s+1}_{i-1}}{\Delta x}.
\end{aligned} \tag{4.11}
$$

This is a fully discretization for (2.10c). Then multiplying equation (4.8) by $\frac{\varepsilon}{c}\mathcal{P}_0$, and adding it to equation (4.3c), sending $\varepsilon \to 0$ and using (4.10), one obtains

$$
\frac{(\rho v_x)^{s+1}_i - (\rho v_x)^s_i}{\Delta t} + \frac{1}{\Delta x}(F^s_{2,i+\frac{1}{2}} - F^s_{2,i-\frac{1}{2}}) + \frac{2\pi\mathcal{P}_0}{3} \frac{J^{s+1}_{i+1} - J^{s+1}_{i-1}}{\Delta x} = 0. \tag{4.12}
$$

This is a fully discretization for (2.10b). Sending $\varepsilon \to 0$ in equation (4.8) and using (4.10) gives

$$
R^{s+1}_i = \frac{4}{c} v^{s+1}_{x,i} J^{s+1}_i - \frac{J^{s+1}_{i+1} - J^{s+1}_{i-1}}{2\Delta x \sigma_{s,i}}, \tag{4.13}
$$

using (4.13) in (4.7) and sending $\varepsilon \to 0$, one gets

$$
\begin{aligned}
4\pi \frac{J^{s+1}_i - J^s_i}{\Delta t} &- \frac{4\pi}{\Delta x}\left[\frac{c}{3\sigma_{s,i+\frac{1}{2}}} \frac{J^{s+1}_{i+1} - J^{s+1}_{i}}{\Delta x} - \frac{c}{3\sigma_{s,i-\frac{1}{2}}} \frac{J^{s+1}_{i} - J^{s+1}_{i-1}}{\Delta x} \right]\\
&+ \frac{16\pi}{3} \frac{v^{s+1}_{x,i+\frac{1}{2}} J^{s+1}_{i+\frac{1}{2}} - v^{s+1}_{x,i-\frac{1}{2}} J^{s+1}_{i-\frac{1}{2}}}{\Delta x} = c\sigma_{a,i}\left((T^{s+1}_i)^4 - 4\pi J^{s+1}_i\right) - \frac{2\pi}{3} v^{s+1}_{x,i} \frac{J^{s+1}_{i+1} - J^{s+1}_{i-1}}{\Delta x},
\end{aligned} \tag{4.14}
$$

which is a fully discretization for (2.10d).

4.3. **Boundary conditions.** In this section, the numerical fluxes in the system (4.3c)–(4.8) under the boundary condition (4.2) are considered. The construction of the flux on the right boundary is similar to the construction on the left boundary, for which we only consider the left boundary case. At the left boundary, the integral representation of the radiative intensity I (A.3) reads:

$$
I_{\frac{1}{2}}(t) = \begin{cases} b_L, & \text{if} \quad n > 0,\\
e^{-\mu_{\frac{1}{2}}(t-t_s)} I\left(t_s, x_{\frac{1}{2}} + \frac{cn}{\varepsilon}(t-t_s)\right) + \frac{1-e^{-\mu_{\frac{1}{2}}(t-t_s)}}{\mu_{\frac{1}{2}}}\widehat{G}_{\frac{1}{2}} & \\
+\int_{t_s}^{t} e^{-\mu_{\frac{1}{2}}(t-t_s)} \left(\frac{c\sigma_{s,\frac{1}{2}}}{\varepsilon^2} J\left(z, x_{\frac{1}{2}} - \frac{cn}{\varepsilon}(t-z)\right) + \frac{c\sigma_{a,\frac{1}{2}}}{4\pi} T^4\left(z, x_{\frac{1}{2}} - \frac{cn}{\varepsilon}(t-z)\right)\right) dz, & \text{if} \quad n < 0. \end{cases} \tag{4.15}
$$

According to the approximation (A.4) and (A.6) , the reconstruction of I for $n<0$ and $x>x_{\frac{1}{2}}$ at the left boundary can be written as:

$$I(t_s,x,n)=I_1^s,$$

and the reconstruction of J for t in the interval $[t_s,t_{s+1}]$:

$$J(t,x)=J_{\frac{1}{2}}^{s+1}+\delta_x J_{\frac{1}{2}}^{s+1,-}(x-x_{\frac{1}{2}}),$$

where $J_{\frac{1}{2}}^{s+1}=\frac{1}{2}(\langle b_L\rangle+J_1^{s+1})$ and $\delta_x J_{\frac{1}{2}}^{s+1,-}=\frac{J_1^{s+1}-J_{\frac{1}{2}}^{s+1}}{\Delta x/2}$. Then the numerical flux at the left boundary reads:

$$\begin{aligned}\zeta_{\frac{1}{2}}=&\frac{cn}{\varepsilon}b_L\mathbb{1}_{n>0}+A_{\frac{1}{2}}nI_1^s\mathbb{1}_{n<0}+C_{\frac{1}{2}}^1 nJ_{\frac{1}{2}}^{s+1}\mathbb{1}_{n<0}+\frac{C_{\frac{1}{2}}^2}{4\pi}n(T_{\frac{1}{2}}^{s+1})^4\mathbb{1}_{n<0}+F_{\frac{1}{2}}n\widehat{G}_{\frac{1}{2}}\mathbb{1}_{n<0}\\&+D_{\frac{1}{2}}^1 n^2\delta_x J_{\frac{1}{2}}^{s+1,-}\mathbb{1}_{n<0}+\frac{D_{\frac{1}{2}}^2}{4\pi}n^2\delta_x(T_{\frac{1}{2}}^{s+1,-})^4\mathbb{1}_{n<0},\end{aligned}$$

which indicates

$$\begin{aligned}\int_{-1}^1\widehat{\zeta}_{\frac{1}{2}}dn=&\int_{-1}^1\left(\frac{cn}{\varepsilon}b_L\mathbb{1}_{n>0}+A_{\frac{1}{2}}nI_1^s\mathbb{1}_{n<0}\right)dn-\frac{1}{2}\left(\frac{C_{\frac{1}{2}}^1}{2}\left(J_1^{s+1}+\langle b_L\rangle\right)+\frac{C_{\frac{1}{2}}^2}{8\pi}((T_1^{s+1})^4+(T_L^{s+1})^4)\right)\\&-\frac{F_{\frac{1}{2}}\widehat{G}_{\frac{1}{2}}}{2}+\frac{1}{3\Delta x}\left(D_{\frac{1}{2}}^1(J_1^{s+1}-\langle b_L\rangle)+\frac{D_{\frac{1}{2}}^2}{4\pi}((T_1^{s+1})^4-(T_L^{s+1})^4)\right),\end{aligned}$$

here T_L^{s+1} is the material temperature at the left boundary, and

$$\begin{aligned}\int_{-1}^1 n\widehat{\zeta}_{\frac{1}{2}}dn=&\int_{-1}^1\left(\frac{cn^2}{\varepsilon}b_L\mathbb{1}_{n>0}+A_{\frac{1}{2}}n^2I_1^s\mathbb{1}_{n<0}\right)dn+\frac{1}{3}\left(\frac{C_{\frac{1}{2}}^1}{2}\left(J_1^{s+1}+\langle b_L\rangle\right)+\frac{C_{\frac{1}{2}}^2}{8\pi}((T_1^{s+1})^4+(T_L^{s+1})^4)\right)\\&+\frac{F_{\frac{1}{2}}\widehat{G}_{\frac{1}{2}}}{3}-\frac{1}{4\Delta x}\left(D_{\frac{1}{2}}^1(J_1^{s+1}-\langle b_L\rangle)+\frac{D_{\frac{1}{2}}^2}{4\pi}((T_1^{s+1})^4-(T_L^{s+1})^4)\right).\end{aligned}$$

To summarize, we have the following one time step update of the fully discrete version of RMHD.

Algorithm 1: one step of fully discrete update for RMHD

Input: ρ_i^s, $v_{x,i}^s$, $v_{y,i}^s$, $v_{z,i}^s$, T_i^s, $B_{y,i}^s$, $B_{z,i}^s$, I_i^s,J_i^s $(J_i^s=\langle I_i^s\rangle)$
Output: ρ_i^{s+1}, $v_{x,i}^{s+1}$, $v_{y,i}^{s+1}$, $v_{z,i}^{s+1}$, T_i^{s+1}, $B_{y,i}^{s+1}$, $B_{z,i}^{s+1}$, I_i^{s+1},J_i^{s+1} $(J_i^{s+1}=\langle I_i^{s+1}\rangle)$

1 obtain ρ_i^{s+1}, $v_{y,i}^{s+1}$, $v_{z,i}^{s+1}$, $B_{y,i}^{s+1}$, $B_{z,i}^{s+1}$ from (4.3b), (4.3d), (4.3e), (4.3g) and (4.3h);
2 obtain R_i^s, Q_i^s from (3.2) and (3.1);
3 get J_i^{s+1}, T_i^{s+1},$v_{x,i}^{s+1}$ and R_i^{s+1} from the system coupled by (4.3c), (4.3f), (4.7) and (4.8);
4 get Q_i^{s+1} from equation (4.3a) and Q_i^s replaced by Q_i^{s+1} and $K_{Q,i}^s$ replaced by $K_{Q,i}^{s+1}$;
5 obtain I_i^{s+1} from (3.1).

5. Numerical Examples

In this section, we conduct numerical experiments to test the performance of our proposed method. The examples cover both optically thin $\varepsilon\sim\mathcal{O}(1)$ and optically thick $\varepsilon\ll 1$ cases, as well as the radiation shock problem. In all the numerical examples, we use S_8 discrete ordinate method in the angle space.

5.1. **Example 1.** In this example, we will test an ideal MHD shock tube problem as in Section V in [2], where $\mathcal{P}_0$=0 in (2.2). In this case, the radiation does not affect the fluid, but the fluid provides source for radiation. The computational domain is $[-1,1]$ and the initial data is given by

$$(\rho, v_x, v_y, v_z, B_y, B_z, p)(x,0) = \begin{cases} (1,0,0,0,1,0,1), & x<0, \\ (0.125,0,0,0,-1,0,0.1), & x>0. \end{cases} \tag{5.1}$$

The magnetic intensity in the x direction $B_x = 0.75$, the ideal gas constant $R_{\text{ideal}} = 1$ and adiabatic index for an ideal gas $\gamma = 2$, the absorption collision cross-section $\sigma_a(x) = 1/3$, the scatter collision cross-section $\sigma_s(x) = 1/3$, $c = 0.1$ and $\varepsilon = 10^{-5}$ in the RMHD system (2.2). The exact solutions at time $t > 0$ involve two fast rarefaction waves, a slow compound wave, a contact discontinuity, and a slow shock. Fig. 1 displays the numerical solutions at $t = 0.2$ obtained by our method using 800 uniform grids. The reference solution is computed by Roe's method shown in [29] with 4000 uniform grids. Moreover, the reference solution of J is solved using the diffusion limit equation (2.10) by the semi-implicit scheme (B.7) and (B.8). For all the schemes, the time step is $\Delta t = 0.2\Delta x$.

5.2. **Example 2.** The uniform accuracy and stability of the AP method at the equilibrium regime are tested in this example. The initial data is the same as in (5.1) in example 1, and the initial temperature and density fluxes are

$$T(0,x) = p/(R_{\text{ideal}}\rho), \qquad I(0,x,n) = \frac{T(0,x)^4}{4\pi}\,. \tag{5.2}$$

Moreover, we assume that $\mathcal{P}_0 = 0.001$, $c = 0.1$ in this example. The absorption collision cross-section σ_a and the scatter collision cross-section σ_s are chosen as $\sigma_a(x) = \sigma_s(x) = 1/3$.

Accuracy. The uniform convergence order of the diffusion limit system (2.14) and the RMHD system (2.11) of our AP scheme are given. In Fig. 3, we plot

$$\begin{aligned}
&\text{error}_\rho = \|\rho_{\Delta x}(\cdot,t_{\max}) - \rho_{\Delta x/2}(\cdot,t_{\max})\|_{l_1}, \quad \text{error}_p = \|p_{\Delta x}(\cdot,t_{\max}) - p_{\Delta x/2}(\cdot,t_{\max})\|_{l_1},\\
&\text{error}_{v_x} = \|(v_x)_{\Delta x}(\cdot,t_{\max}) - (v_x)_{\Delta x/2}(\cdot,t_{\max})\|_{l_1}, \qquad \text{error}_{v_y} = \|(v_y)_{\Delta x}(\cdot,t_{\max}) - (v_y)_{\Delta x/2}(\cdot,t_{\max})\|_{l_1},\\
&\text{error}_{B_y} = \|(B_y)_{\Delta x}(\cdot,t_{\max}) - (B_y)_{\Delta x/2}(\cdot,t_{\max})\|_{l_1}, \qquad \text{error}_T = \|T_{\Delta x}(\cdot,t_{\max}) - T_{\Delta x/2}(\cdot,t_{\max})\|_{l_1},
\end{aligned} \tag{5.3}$$

for the diffusion limit system (2.14) with decreasing Δx and $t_{\max} = 0.2$. Then in Figs. 4, we plot the same errors for RMHD system (2.11) with decreasing Δx and $t_{\max} = 0.2$ for different values of $\varepsilon = 1$,10^{-1}, 10^{-3}, 10^{-5}.

Stability condition. To check the stability, we choose $\Delta t = C\Delta x$ with C being constant, and record the largest possible choice of C in Table 1 for different ε and Δx. Uniform hyperbolic stability is observed numerically.

Table 1. Stability test for the RMHD system (2.11). Here we use $\Delta t = C\Delta x$ and the largest possible C that stabilize the scheme are displayed.

ε \ Δx	$\frac{1}{100}$	$\frac{1}{200}$	$\frac{1}{400}$	$\frac{1}{800}$	$\frac{1}{1600}$
1	0.2	0.2	0.2	0.2	0.2
0.1	0.2	0.2	0.2	0.2	0.2
1e-03	0.2	0.2	0.2	0.2	0.2
1e-05	0.2	0.2	0.2	0.2	0.2

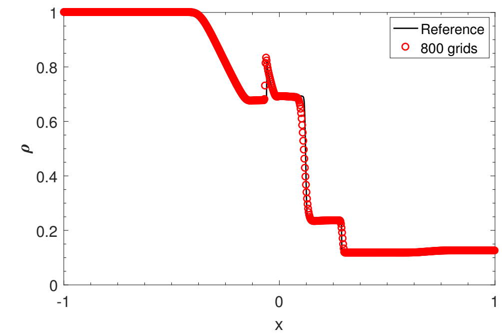

(a) Density ρ

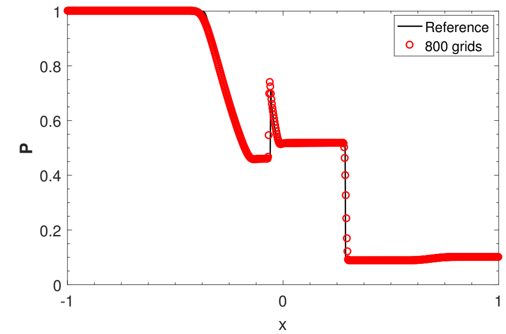

(b) Pressure p

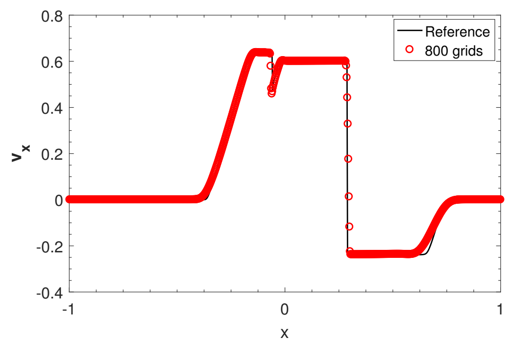

(c) Velocity in x-direction v_x

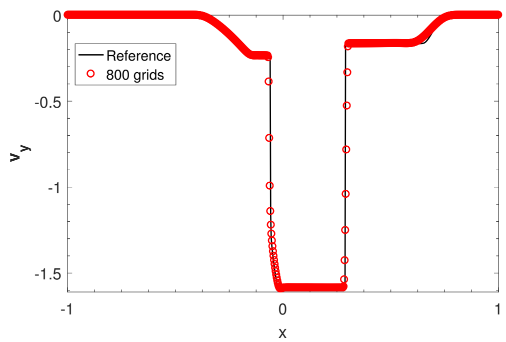

(d) Velocity in y-direction v_y

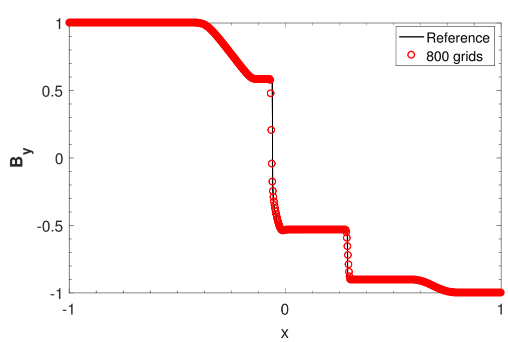

(e) Magnetic field in y-direction B_y

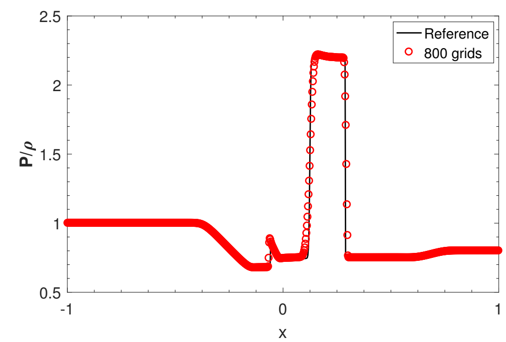

(f) The ratio of the pressure and the density

FIGURE 1. The numerical results at time $t = 0.2$ using our method with 800 grids points in space (squares) and the Roe solver with 4,000 grids points in space (solid line). For both schemes, $\Delta t = 0.2\Delta x$.

Comparison with reference solutions. We consider two cases with $\varepsilon = 1$ and $\varepsilon = 10^{-5}$ as in [3]. To compute the reference solution with $\varepsilon = 1$, use a fully resolved explicit finite volume solver. For $\varepsilon \ll 1$, we solve the diffusion limit equation (2.10) by the semi-implicit scheme (B.7) and (B.8). The results are shown in Fig. 5 and Fig. 6. We can see that our results agree well with the reference solutions.

5.3. **Example 3.** In the simulation of RMHD, it is a challenging task to produce accurate radiative shocks, especially in the optically thick regime. We test a range of the radiation-hydrodynamic shock problems presented in [20] in which several shocks are presented in the solution. For each of these shocks, we set $\mathcal{P}_0 = 10^{-4}$, adiabatic index for an ideal gas $\gamma = 5/3$, absorption collision cross-section $\sigma_a = 1/3$, scatter

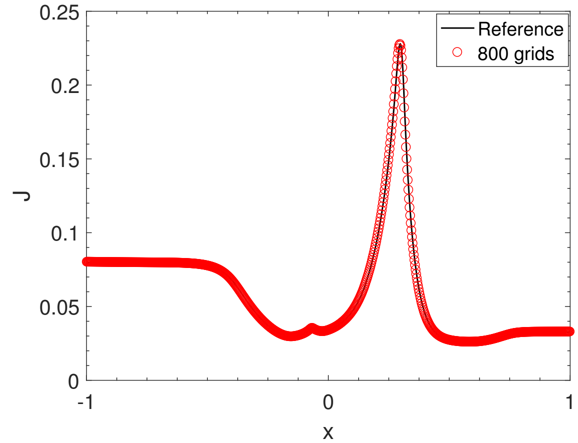

FIGURE 2. Comparison of J of our AP scheme and the reference solution obtained by semi-implicit solver (B.7)–(B.8) for RMHD system (2.2). Here $\mathcal{P}_0 = 0$, $\varepsilon = 10^{-5}$, $t = 0.2$, $\Delta x = 1/800$, $\Delta t = 0.2\Delta x$ for both two schemes.

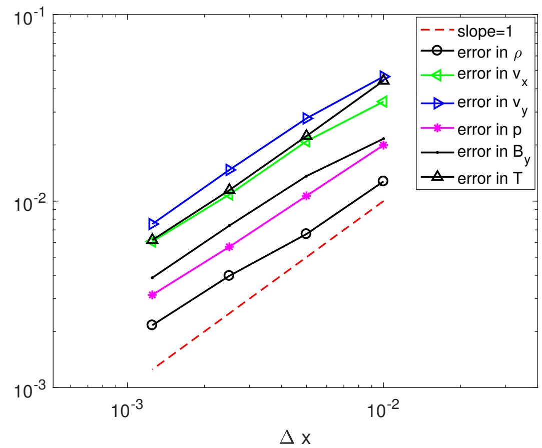

FIGURE 3. Plot of errors (5.3) for diffusion limit system (2.14) with decreasing $\Delta x = \frac{1}{100}$, $\frac{1}{200}$, $\frac{1}{400}$, $\frac{1}{800}$, $\frac{1}{1600}$. Here $\Delta t = 0.2\Delta x$.

collision cross-section $\sigma_s = 10^6$, $c = 3 \times 10^6$, $\varepsilon = 1$ in RMHD system (2.2), and the radiation temperature $T_r \equiv (4\pi J)^{0.25}$. Moreover, the computational domain is $[-0.02, 0.02]$ and the results at $t = 0.04$ are displayed. In this example, $\Delta x = 1/800$, $\Delta t = 0.2\Delta x$. In [20], the authors have obtained some semi-analytic solutions for the non-equilibrium diffusion limit system (2.10) at different Mach numbers, we compare the numerical results with the semi-analytic solutions obtained [20].

$$(\rho, v_x, v_y, v_z, B_y, B_z, T, T_r)(x, 0) = \begin{cases} (1, 1.2, 0, 0, 0, 0, 1, 1), & x < 0, \\ (1.298088, 0.9244363, 0, 0, 0, 0, 1.194888, 1.194888), & x > 0, \end{cases} \tag{5.4}$$

$$(\rho, v_x, v_y, v_z, B_y, B_z, T, T_r)(x, 0) = \begin{cases} (1, 2, 0, 0, 0, 0, 1, 1), & x < 0, \\ (2.287066, 0.874482876, 0, 0, 0, 0, 2.077223, 2.077223), & x > 0. \end{cases} \tag{5.5}$$

First of all, a Mach 1.2 shock is considered, which has no isothermal sonic point (ISP) but a hydrodynamic shock. The initial conditions are shown in (5.4). Fig. 7 compares our numerical results with the semi-analytic

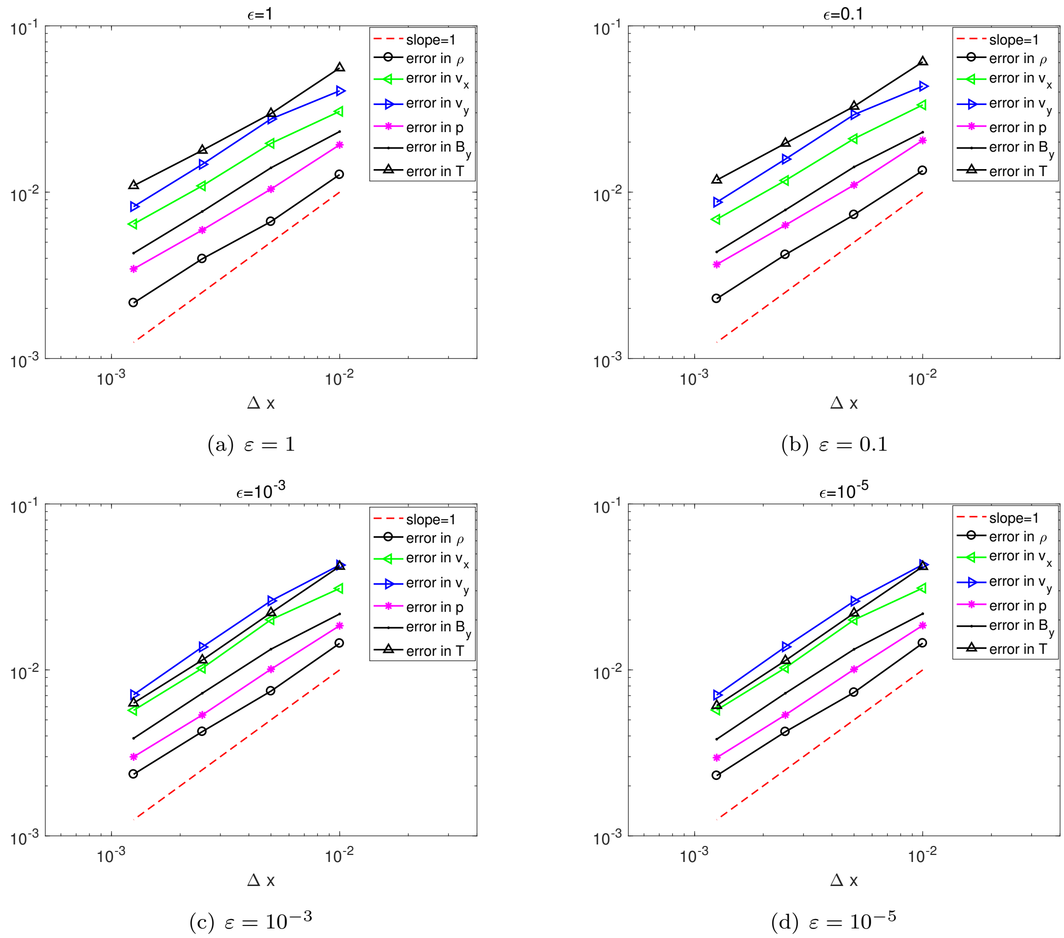

FIGURE 4. Plot of errors (5.3) for RMHD system (2.11) with decreasing $\Delta x = \frac{1}{100}, \frac{1}{200}, \frac{1}{400}, \frac{1}{800}, \frac{1}{1600}$. Here $\Delta t = 0.2\Delta x$, $\varepsilon = 1, 0.1, 10^{-3}$ and 10^{-5}.

solutions, in which we can see good agreement for all quantities, including density, velocity, material and radiation temperature. Due to the hydrodynamic shock, there exhibits discontinuities in the solution profiles of density, velocity and material temperature, and the maximum material temperature is bounded, since there is no ISP to drive it further.

At Mach 2, there are both a hydrodynamic shock and an ISP. The initial conditions are given in (5.5). Fig. 8 compares our numerical results with the semi-analytic solutions. One can see that our numerical results are in good agreement with the semi-analytic solutions. In Fig. 8, discontinuities can be seen in material density, velocity and material temperature due to the hydrodynamic shock. Moreover, the Zel'dovich spike can be observed in material temperature as in Fig. 8(c). The Zel'dovich spike is caused by the ISP embedded within the hydrodynamic shock, which drives up the material temperature at the shock front.

6. CONCLUSION AND DISCUSSIONS

In this paper, we have introduced an AP scheme in both space and time for the RMHD system that couples the ideal MHD equations with a gray RTE, and two different scalings are considered, one results in an equilibrium diffusion limit system, while the other results in nonequilibrium. The main idea is to decompose the intensity into three parts, two parts correspond to the zeroth and first order moments, while

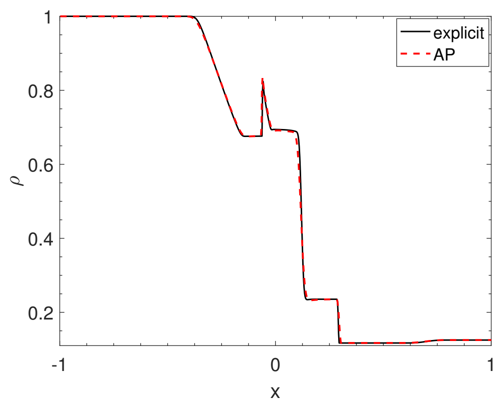

(a) Density ρ

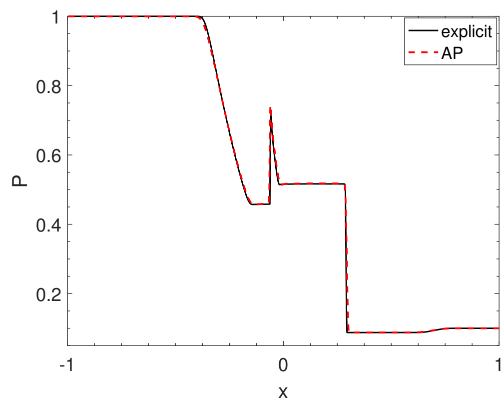

(b) Pressure p

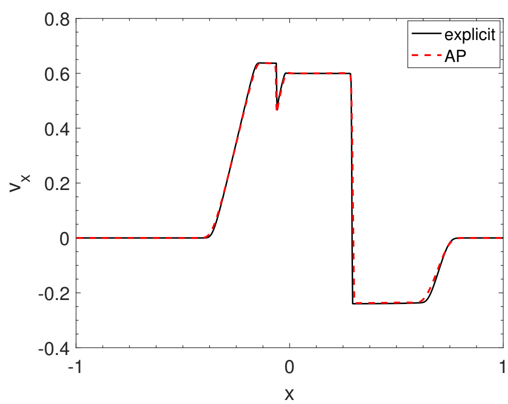

(c) Velocity in x-direction v_x

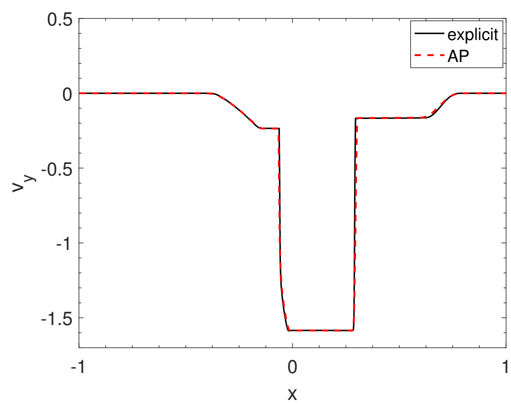

(d) Velocity in y-direction v_y

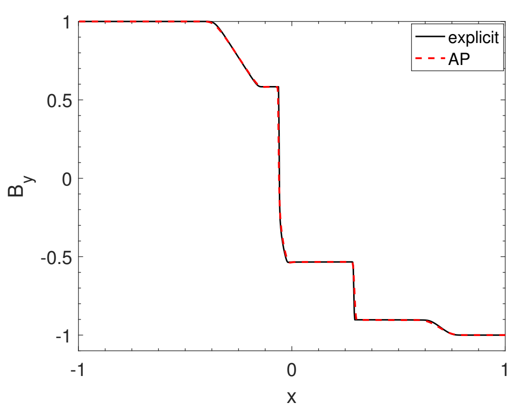

(e) Magnetic field in y-direction B_y

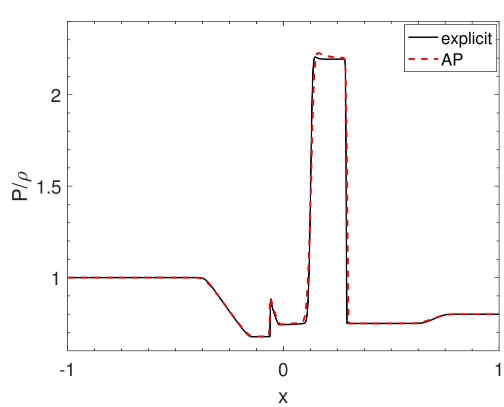

(f) The ratio of the pressure and the density

FIGURE 5. Comparison of the results of our AP scheme and the reference solution obtained by fully explicit scheme for RMHD system (2.11). Here $\varepsilon = 1$, $t = 0.2$, $\Delta x = 1/800$, $\Delta t = 0.2\Delta x$ for the AP scheme, and $\Delta x = 1/4000$, $\Delta t = 0.001\Delta x$ for the explicit solver.

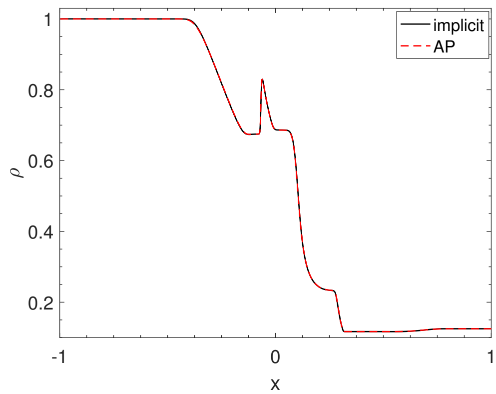

(a) Density ρ

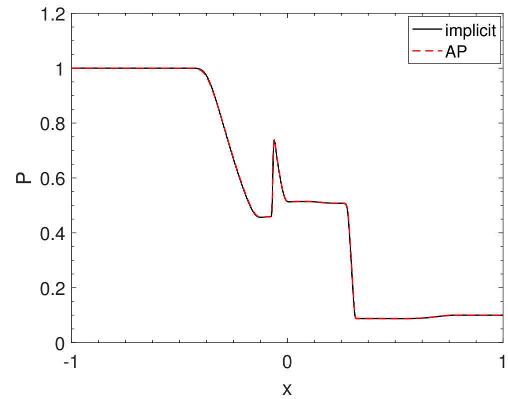

(b) Pressure p

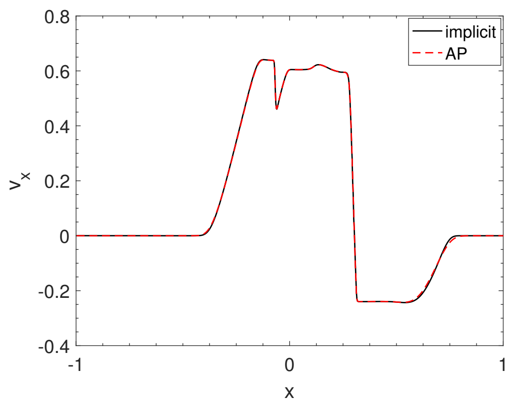

(c) Velocity in x-direction v_x

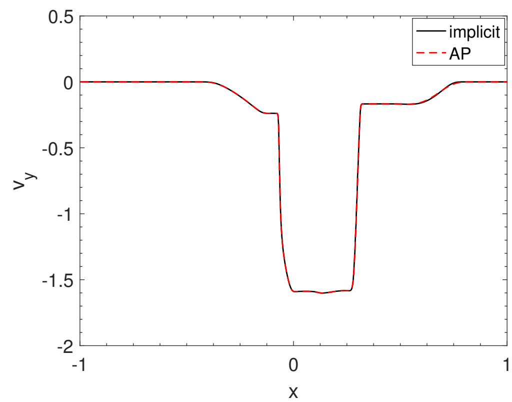

(d) Velocity in y-direction v_y

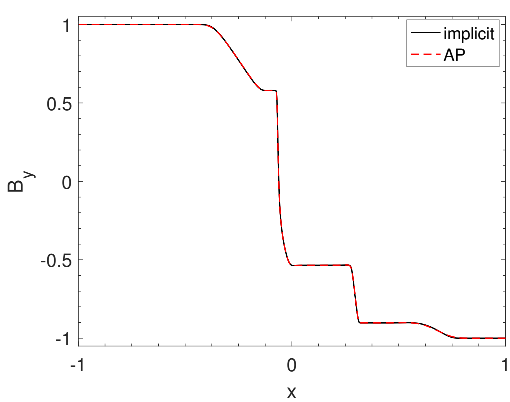

(e) Magnetic field in y-direction B_y

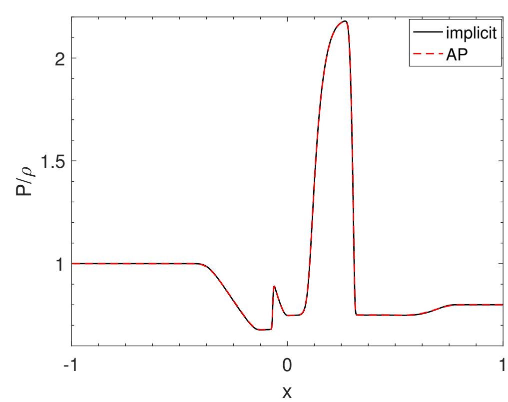

(f) The ratio of the pressure and the density

FIGURE 6. Comparison of the results of our AP scheme and the reference solution obtained by the semi-implicit solver (B.7)–(B.8) for RMHD system (2.11). Here $\varepsilon = 10^{-5}$, $t = 0.2$, $\Delta x = 1/800$, $\Delta t = 0.2\Delta x$ for both two schemes.

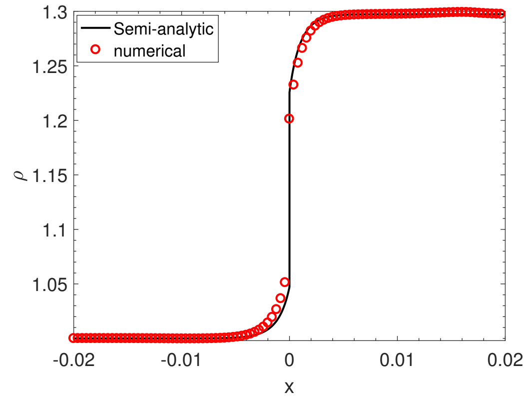

(a) Density ρ

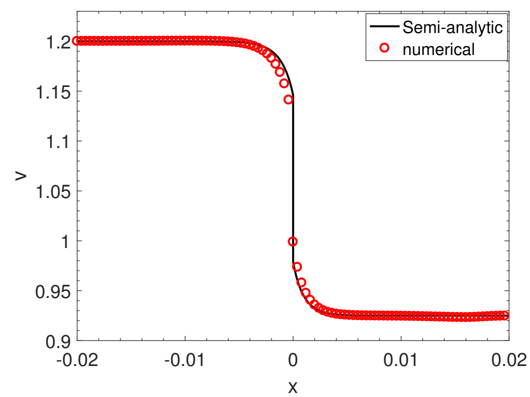

(b) Velocity v

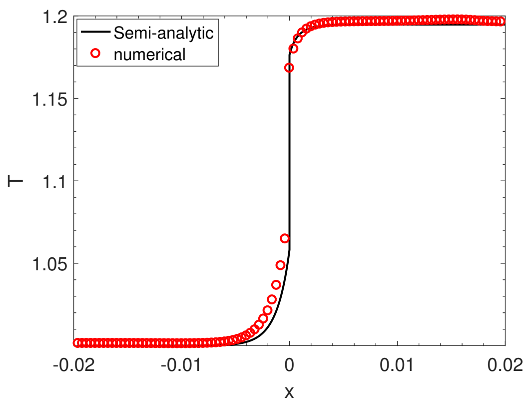

(c) Temperature T

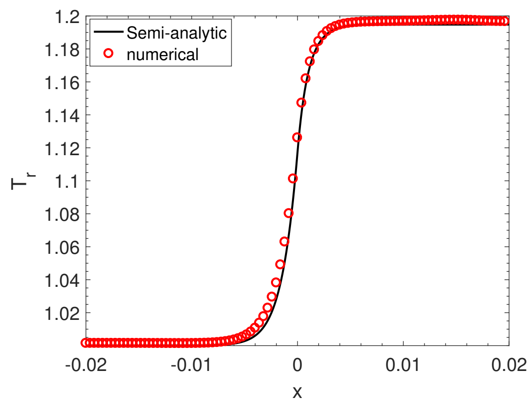

(d) Radiation temperature T_r

FIGURE 7. Comparison of the results using our AP scheme at time $t = 0.04$ and the semi-analytic solution for Mach number $\mathcal{M} = 1.2$. For AP scheme, we use $\Delta x = 1/800$ and $\Delta t = 0.2\Delta x$.

the third part is the residual. The two macroscopic moments are treated implicitly while the residual is explicit. For the space discretization, we use Roe's method in the Athena code to solve the convective part in the ideal MHD equations and the UGKS for the RTE. Numerical results are presented in the optically thick region and the radiative shock problem, which are compared to the semi-analytic solution to verify accuracy and asymptotic properties of our method.

It would be worthwhile to construct a second-order AP method for the radiation magnetohydrodynamics system. In the semi-implicit scheme, a simple time-integration method has been used. To obtain a second scheme, higher order IMEX time-integration method can be considered.

Acknowledgement: The authors would like to thank Dr. Yanfei Jiang from Computational Center for Astrophysics, the Flatiron Institute, for proposing this problem and useful discussions. S. Jin is partially supported by NSFC12031013 and the Strategic Priority Research Program of Chinese Academy of Sciences, XDA25010404; M. Tang and X. J. Zhang are partially supported by NSFC11871340 and the Strategic Priority Research Program of Chinese Academy of Sciences, XDA25010401.

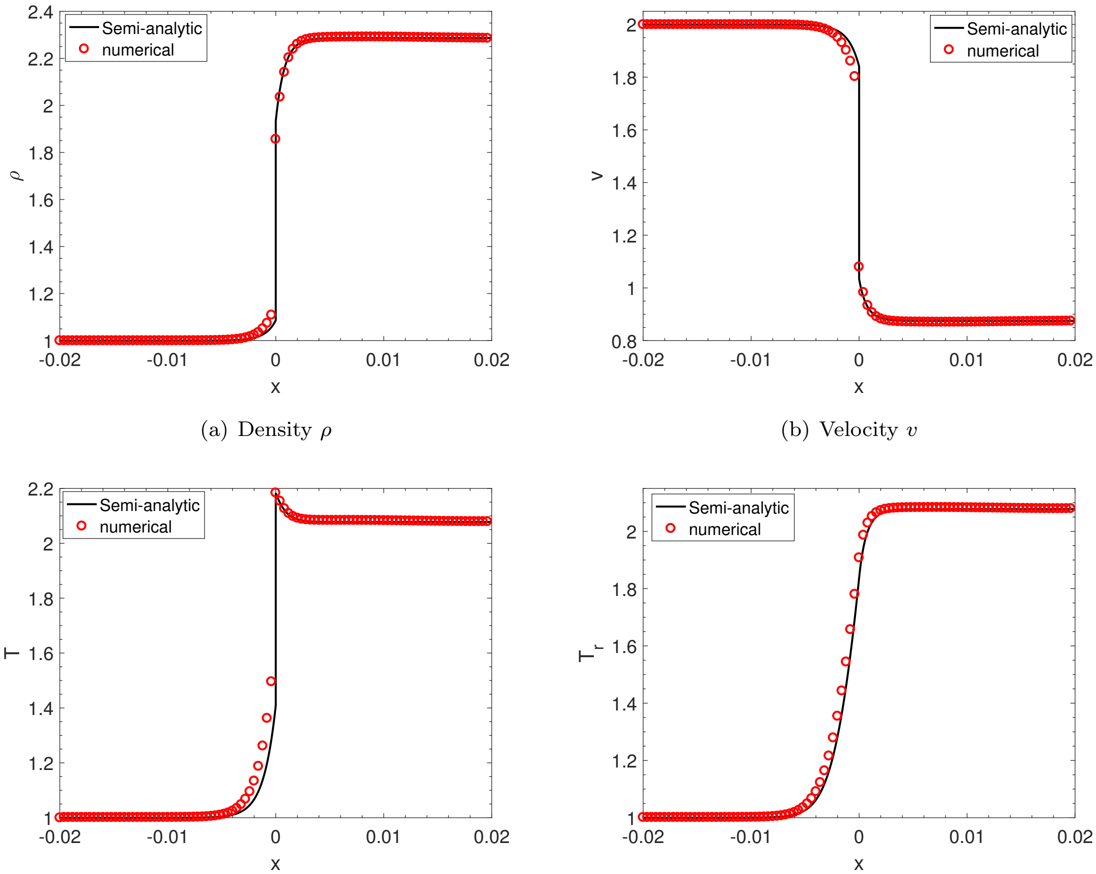

(a) Density ρ

(b) Velocity v

(c) Temperature T

(d) Radiation temperature T_r

FIGURE 8. Comparison of the results using our AP scheme at time $t = 0.04$ and the semi-analytic solution for Mach number $\mathcal{M} = 2$. For AP scheme, we use $\Delta x = 1/800$ and $\Delta t = 0.2\Delta x$.

APPENDIX A. THE PROCESSES OF UGKS FOR THE NON-EQUILIBRIUM REGIME

Recall the RTE (4.1a) in the slab geometry, and integrating it over $[t_s, t_{s+1}]$ and $[x_{i-\frac{1}{2}}, x_{1+\frac{1}{2}}]$ gives

$$\frac{I_i^{s+1} - I_i^s}{\Delta t} + \frac{1}{\Delta x}(\zeta_{i+\frac{1}{2}} - \zeta_{i-\frac{1}{2}}) = c\sigma_{a,i}\left(\frac{(T_i^{s+1})^4}{4\pi} - I_i^{s+1}\right) + \frac{c\sigma_{s,i}}{\varepsilon^2}(J_i^{s+1} - I_i^{s+1}) + G.$$

The microscopic flux ζ is computed by solving the following initial value problem at the cell boundary $x = x_{i+\frac{1}{2}}$:

$$\begin{cases} \dfrac{I_i^{s+1} - I_i^s}{\Delta t} + \dfrac{1}{\Delta x}(\zeta_{i+\frac{1}{2}} - \zeta_{i-\frac{1}{2}}) = c\sigma_{a,i}\left(\dfrac{(T_i^{s+1})^4}{4\pi} - I_i^{s+1}\right) + \dfrac{c\sigma_{s,i}}{\varepsilon^2}(J_i^{s+1} - I_i^{s+1}) + G, \\ I(t,x,n)|_{t=t_s} = I(t_s, x, n). \end{cases} \tag{A.1}$$

In the UGKS scheme, we firstly assume the coefficients σ_a and σ_s in space and time are piecewise constant, thus the radiative transfer equation in RMHD system (4.1) is equivalent to

$$\frac{d}{dt}e^{\mu t} I\left(t, x + \frac{cn}{\varepsilon}t, n\right) = e^{\mu t}\left(\frac{c\sigma_s}{\varepsilon^2} J\left(t, x + \frac{cn}{\varepsilon}t, n\right) + \frac{c\sigma_a}{4\pi} T^4\left(t, x + \frac{cn}{\varepsilon}t, n\right) + G\right), \tag{A.2}$$

with $\mu = \frac{\varepsilon^2 c\sigma_a + c\sigma_s}{\varepsilon^2}$. Solving the equivalent equation (A.2) with the initial value in the system (A.1), which gives the solution

$$\begin{aligned} I(t, x_{i+\frac{1}{2}}, n) \approx\, & e^{-\mu_{i+\frac{1}{2}}(t-t_s)} I\left(t_s, x_{i+\frac{1}{2}} + \frac{cn}{\varepsilon}(t-t_s)\right) + \frac{1-e^{-\mu_{i+\frac{1}{2}}(t-t_s)}}{\mu_{i+\frac{1}{2}}} \widehat{G}_{i+\frac{1}{2}} \\ & + \int_{t_s}^{t} e^{-\mu_{i+\frac{1}{2}}(t-t_s)} \left(\frac{c\sigma_{s,i+\frac{1}{2}}}{\varepsilon^2} J\left(z, x_{i+\frac{1}{2}} - \frac{cn}{\varepsilon}(t-z)\right) + \frac{c\sigma_{a,i+\frac{1}{2}}}{4\pi} T^4\left(z, x_{i+\frac{1}{2}} - \frac{cn}{\varepsilon}(t-z)\right)\right) dz, \end{aligned} \tag{A.3}$$

with $\mu_{i+\frac{1}{2}}$, $\sigma_{a,i+\frac{1}{2}}$ and $\sigma_{s,i+\frac{1}{2}}$ being the constant value at the corresponding cell boundary for μ, σ_a and σ_s respectively. In solution (A.3), there remains three terms that need to approximate: the first one is the initial condition $I(t_s)$ around $x_{i+\frac{1}{2}}$, namely the function $I\left(t_s, x_{i+\frac{1}{2}} + \frac{cn}{\varepsilon}(t-t_s)\right)$; the second one is the two functions J, T^4 localized in the time interval $[t_s, t_{s+1}]$ and around the boundary $x_{i+\frac{1}{2}}$, i.e., the functions $J\left(z, x_{i+\frac{1}{2}} - \frac{cn}{\varepsilon}(t-z)\right)$ and $T^4\left(z, x_{i+\frac{1}{2}} - \frac{cn}{\varepsilon}(t-z)\right)$; the last one is the term $\widehat{G}_{i+\frac{1}{2}}$.

The first term: For the first term, a piecewise linear reconstruction function is used to approximate the initial function $I(t_s)$ around $x_{i+\frac{1}{2}}$:

$$I(t_s, x, n) = \begin{cases} I_i^s + \delta_x I_i^s (x - x_i), & \text{if} \quad x < x_{i+\frac{1}{2}}, \\ I_{i+1}^s + \delta_x I_{i+1}^s (x - x_{i+1}), & \text{if} \quad x > x_{i+\frac{1}{2}}. \end{cases} \tag{A.4}$$

Here $\delta_x I_i^s$ is the limited slope determined by the minmod limiter [26]:

$$\delta_x I_i^s = \begin{cases} \min\{\frac{I_{i+1}^s - I_i^s}{\Delta x}, \frac{I_{i+1}^s - I_{i-1}^s}{2\Delta x}, \frac{I_i^s - I_{i-1}^s}{\Delta x}\}, & \text{if all are positive}, \\ \max\{\frac{I_{i+1}^s - I_i^s}{\Delta x}, \frac{I_{i+1}^s - I_{i-1}^s}{2\Delta x}, \frac{I_i^s - I_{i-1}^s}{\Delta x}\}, & \text{if all are negative}, \\ 0, & \text{otherwise}. \end{cases} \tag{A.5}$$

The second term: For the second term, the approximations of two functions J and T^4 between t_s and t_{s+1} and around $x_{i+\frac{1}{2}}$ are constructed in the same manner, so only the approximation of J is introduced in detail. The function J is treated implicitly in time by using piecewise linear polynomials, so the reconstruction for J reads:

$$J(t, x) = \begin{cases} J_{i+\frac{1}{2}}^{s+1} + \delta_x J_{i+\frac{1}{2}}^{s+1,+} (x - x_{i+\frac{1}{2}}), & \text{if} \quad x < x_{i+\frac{1}{2}}, \\ J_{i+\frac{1}{2}}^{s+1} + \delta_x J_{i+\frac{1}{2}}^{s+1,-} (x - x_{i+\frac{1}{2}}), & \text{if} \quad x > x_{i+\frac{1}{2}}, \end{cases} \tag{A.6}$$

with the interface value of J defined by

$$J_{i+\frac{1}{2}}^{s+1} = \left\langle I_{i+\frac{1}{2}}^{s+1}(n) \right\rangle = \frac{1}{2} \left\langle I_i^{s+1} + I_{i+1}^{s+1} \right\rangle,$$

and with the spatial derivatives given by

$$\delta_x J_{i+\frac{1}{2}}^{s+1,+} = \frac{J_{i+\frac{1}{2}}^{s+1} - J_i^{s+1}}{\Delta x/2}, \quad \delta_x J_{i+\frac{1}{2}}^{s+1,-} = \frac{J_{i+1}^{s+1} - J_{i+\frac{1}{2}}^{s+1}}{\Delta x/2}.$$

The third term: At last, the approximation for the term $\widehat{G}$ is discussed. Recall the definition of G_i:

$$\begin{aligned} G_i =& 3\varepsilon\sigma_{a,i} n v_{x,i}^{s+1} \left(\frac{(T_i^{s+1})^4}{4\pi} - J_i^{s+1} \right) + n v_{x,i}^{s+1} \left(\varepsilon\sigma_{a,i} + \frac{\sigma_{s,i}}{\varepsilon} \right) \left(4J_i^{s+1} + \varepsilon(nR_i^{s+1} + Q_i^s) \right) \\ & - \frac{2}{3}\sigma_{s,i} v_{x,i}^{s+1} R_i^{s+1} - \frac{(\varepsilon^2\sigma_{a,i} - \sigma_{s,i})(v_{x,i}^{s+1})^2}{c} \left(\frac{4}{3} J_i^{s+1} + \varepsilon K_{Q,i}^s \right), \end{aligned}$$

The upwind scheme is used to determine $\widehat{G}$, i.e., the value of $\widehat{G}$ at the center of the interval $[x_i, x_{i+1}]$ is determined by the velocity field v at the both sides boundary,

$$\begin{cases} \text{If } v_{x,i}^{s+1} \geq v_{x,i+1}^{s+1}: \\ \widehat{G}_{i+\frac{1}{2}} = G_i, \quad \text{if } \left(G_{i+1} - G_i\right) / \left(v_{x,i+1}^{s+1} - v_{x,i}^{s+1}\right) > 0, \\ \widehat{G}_{i+\frac{1}{2}} = G_{i+1}, \quad \text{if } \left(G_{i+1} - G_i\right) / \left(v_{x,i+1}^{s+1} - v_{x,i}^{s+1}\right) \leq 0; \\ \text{If } v_{x,i}^{s+1} < v_{x,i+1}^{s+1}: \\ \widehat{G}_{i+\frac{1}{2}} = G_i, \quad \text{if } v_{x,i}^{s+1} > 0, \\ \widehat{G}_{i+\frac{1}{2}} = G_{i+1}, \quad \text{if } v_{x,i+1}^{s+1} < 0, \\ \widehat{G}_{i+\frac{1}{2}} = 0, \quad \text{if } v_{x,i}^{s+1} \leq 0 \leq v_{x,i+1}^{s+1}. \end{cases} \tag{A.7}$$

Appendix B. The full discretization for the equilibrium regime

Here, we will show the full discretization for system (2.11). Applying semi-implicit finite volume scheme in system (2.11), the fully discretization of (2.11) is same with (4.3) except the RTE and source terms S_{re} and S_{rp}, which read:

$$\begin{aligned} \frac{J_i^{s+1} - J_i^s}{\Delta t} + \varepsilon \frac{nR_i^{s+1} + Q_i^{s+1} - nR_i^s - Q_i^s}{\Delta t} + \frac{1}{\Delta x}(\widetilde{\zeta}_{i+\frac{1}{2}} - \widetilde{\zeta}_{i-\frac{1}{2}}) = \frac{c\sigma_{a,i}}{\varepsilon^2}\left(\frac{(T_i^{s+1})^4}{4\pi} - J_i^{s+1}\right) \\ - \left(\frac{c\sigma_{a,i}}{\varepsilon} + c\varepsilon\sigma_{s,i}\right)(nR_i^{s+1} + Q_i^{s+1}) + \widetilde{G}_i, \end{aligned}$$

with the source term:

$$\begin{aligned} \widetilde{G}_i =& 3\frac{\sigma_{a,i}}{\varepsilon} n v_{x,i}^{s+1}\left(\frac{(T_i^{s+1})^4}{4\pi} - J_i^{s+1}\right) + n v_{x,i}^{s+1}\left(\frac{\sigma_{a,i}}{\varepsilon} + \varepsilon\sigma_{s,i}\right)\left(4J_i^{s+1} + \varepsilon(nR_i^{s+1} + Q_i^s)\right) \\ & - \frac{2}{3}\varepsilon^2\sigma_{s,i} v_{x,i}^{s+1} R_i^{s+1} - \frac{(\sigma_{a,i} - \varepsilon^2\sigma_{s,i})(v_{x,i}^{s+1})^2}{c}\left(\frac{4}{3}J_i^{s+1} + \varepsilon K_{Q,i}^s\right), \end{aligned}$$

and

$$(\widetilde{S_{re}})_i^{s+1} = 4\pi\frac{\sigma_{a,i}}{\varepsilon}\left(\frac{(T_i^{s+1})^4}{4\pi} - J_i^{s+1}\right) + \frac{4\pi(\varepsilon\sigma_{a,i} - \varepsilon^3\sigma_{s,i})v_{x,i}^{s+1}}{c^2}\left[\frac{c}{3}R_i^{s+1} - v_{x,i}^{s+1}\left(\frac{4}{3}J_i^{s+1} + \varepsilon K_{Q,i}^s\right)\right],$$

$$(\widetilde{S_{rp}})_i^{s+1} = -\frac{4\pi(\varepsilon^2\sigma_{s,i} + \sigma_{a,i})}{c}\left[\frac{c}{3}R_i^{s+1} - v_{x,i}^{s+1}\left(\frac{4}{3}J_i^{s+1} + \varepsilon K_{Q,i}^s\right)\right] + \frac{4\pi\sigma_{a,i}v_{x,i}^{s+1}}{c}\left(\frac{(T_i^{s+1})^4}{4\pi} - J_i^{s+1}\right).$$

Moreover, the numerical flux $\widetilde{\zeta}_{i+\frac{1}{2}}$ is defined by

$$\begin{aligned} \widetilde{\zeta}_{i+\frac{1}{2}} = & A_{i+\frac{1}{2}} n\left(I_{i+\frac{1}{2}}^{s,+}\mathbb{1}_{n>0} + I_{i+\frac{1}{2}}^{s,-}\mathbb{1}_{n<0}\right) + C_{i+\frac{1}{2}}^1 nJ_{i+\frac{1}{2}}^{s+1} + \frac{C_{i+\frac{1}{2}}^2}{4\pi}n(T_{i+\frac{1}{2}}^{s+1})^4 + F_{i+\frac{1}{2}} n\breve{G}_{i+\frac{1}{2}} \\ & + D_{i+\frac{1}{2}}^1 n^2\left(\delta_x J_{i+\frac{1}{2}}^{s+1,+}\mathbb{1}_{n>0} + \delta_x J_{i+\frac{1}{2}}^{s+1,-}\mathbb{1}_{n<0}\right) + \frac{D_{i+\frac{1}{2}}^2}{4\pi}n^2\left(\delta_x(T_{i+\frac{1}{2}}^{s+1,+})^4\mathbb{1}_{n>0} + \delta_x(T_{i+\frac{1}{2}}^{s+1,-})^4\mathbb{1}_{n<0}\right), \end{aligned} \tag{B.1}$$

where the coefficients in the numerical flux are given by:

$$\begin{aligned}
&A = \frac{c}{\Delta t \varepsilon \mu}(1-e^{-\mu\Delta t}),\\
&C^1 = \frac{c^2\sigma_s}{\Delta t\varepsilon\mu}\left(\Delta t - \frac{1}{\mu}(1-e^{-\mu\Delta t})\right), \qquad C^2 = \frac{c^2\sigma_a}{\Delta t\varepsilon^3\mu}\left(\Delta t - \frac{1}{\mu}(1-e^{-\mu\Delta t})\right),\\
&D^1 = -\frac{c^3\sigma_s}{\Delta t\varepsilon^2\mu^2}\left(\Delta t\left(1+e^{-\mu\Delta t}\right) - \frac{2}{\mu}\left(1-e^{-\mu\Delta t}\right)\right),\\
&D^2 = -\frac{c^3\sigma_a}{\Delta t\varepsilon^4\mu^2}\left(\Delta t\left(1+e^{-\mu\Delta t}\right) - \frac{2}{\mu}\left(1-e^{-\mu\Delta t}\right)\right),\\
&F = \frac{c}{\Delta t\varepsilon\mu}\left(\Delta t - \frac{1}{\mu}\left(1-e^{-\mu\Delta t}\right)\right),
\end{aligned} \tag{B.2}$$

with $\mu = \frac{c\sigma_a+\varepsilon^2 c\sigma_s}{\varepsilon^2}$, and $\breve{G}_{i+\frac12}$ is defined in the same way with $\widehat{G}_{i+\frac12}$. Moreover, the zeroth and first moments of (B.1) are:

$$4\pi\frac{J_i^{s+1}-J_i^s}{\Delta t} + \frac{2\pi}{\Delta x}\int_{-1}^1 \widetilde{\zeta}_{i+\frac12} - \widetilde{\zeta}_{i-\frac12}\,dn = \frac{c}{\varepsilon}(\widetilde{S_{re}})_i^{s+1}, \tag{B.3}$$

where

$$\begin{aligned}
\int_{-1}^1 \widetilde{\zeta}_{i+\frac12}\,dn =& \int_{-1}^1 A_{i+\frac12} n\left(I^{s,+}_{i+\frac12}\mathbb{1}_{n>0} + I^{s,-}_{i+\frac12}\mathbb{1}_{n<0}\right)dn + \frac{2D^1_{i+\frac12}}{3}\frac{J^{s+1}_{i+1}-J^{s+1}_i}{\Delta x} + \frac{D^2_{i+\frac12}}{6\pi}\frac{(T^{s+1}_{i+1})^4-(T^{s+1}_i)^4}{\Delta x}\\
&+F_{i+\frac12}\left[2\frac{\sigma_{a,i+\frac12}}{\varepsilon}v^{s+1}_{x,i+\frac12}\left(\frac{(T^{s+1}_{i+\frac12})^4}{4\pi} - J^{s+1}_{i+\frac12}\right) + v^{s+1}_{x,i+\frac12}\frac{\sigma_{a,i+\frac12}+\varepsilon^2\sigma_{s,i+\frac12}}{\varepsilon}\left(\frac{8}{3}J^{s+1}_{i+\frac12} + 2\varepsilon K^s_{Q,i+\frac12}\right)\right],
\end{aligned}$$

$$\frac{4\pi\varepsilon}{3}\frac{R_i^{s+1}-R_i^s}{\Delta t} + \frac{2\pi}{\Delta x}\int_{-1}^1 n\left(\widetilde{\zeta}_{i+\frac12} - \widetilde{\zeta}_{i-\frac12}\right)dn = \frac{c}{\varepsilon}(\widetilde{S_{rp}})_i^{s+1}, \tag{B.4}$$

where

$$\begin{aligned}
\int_{-1}^1 n\widetilde{\zeta}_{i+\frac12}\,dn =& \int_{-1}^1 A_{i+\frac12} n^2\left(I^{s,+}_{i+\frac12}\mathbb{1}_{n>0} + I^{s,-}_{i+\frac12}\mathbb{1}_{n<0}\right)dn + \frac{C^1_{i+\frac12}}{3}(J^{s+1}_{i+1}+J^{s+1}_i) + \frac{C^2_{i+\frac12}}{12\pi}((T^{s+1}_{i+1})^4+(T^{s+1}_i)^4)\\
&+F_{i+\frac12}\left[v^{s+1}_{x,i+\frac12}\left(\varepsilon^2\sigma_{s,i+\frac12}+\sigma_{a,i+\frac12}\right)\left(\frac{2}{5}R^{s+1}_{i+\frac12} + \int_{-1}^1 n^3 Q^s_{i+\frac12}\,dn\right) - \frac{4}{9}\varepsilon^2\sigma_{s,i+\frac12}v^{s+1}_{x,i+\frac12}R^{s+1}_{i+\frac12}\right.\\
&\left.-\frac{2(\sigma_{a,i+\frac12}-\varepsilon^2\sigma_{s,i+\frac12})(v^{s+1}_{x,i+\frac12})^2}{3c}\left(\frac{4}{3}J^{s+1}_{i+\frac12} + \varepsilon K^s_{Q,i+\frac12}\right)\right].
\end{aligned}$$

At last, we will give the diffusion limit of the full discretization of the equilibrium case. Firstly, assuming σ_a and σ_s are positive, as $\varepsilon \to 0$, the leading order of the coefficients in the numerical flux (B.1) are

$$\begin{aligned}
&A(\Delta t, \varepsilon, c, \sigma_a, \sigma_s) = 0 + \mathcal{O}(\varepsilon),\\
&\varepsilon C^1(\Delta t, \varepsilon, c, \sigma_a, \sigma_s) = 0 + \mathcal{O}(\varepsilon), \qquad \varepsilon C^2 = c + \mathcal{O}(\varepsilon),\\
&D^1 = 0 + \mathcal{O}(\varepsilon), \qquad D^2 = -\frac{c}{\sigma_a} + \mathcal{O}(\varepsilon),\\
&\frac{1}{\varepsilon}F = \frac{1}{\sigma_a} + \mathcal{O}(\varepsilon).
\end{aligned}$$

which means the zero moment and the first moment of the numerical flux, as $\varepsilon \to 0$, have the following limit:

$$\int_{-1}^1 \widehat{\zeta}_{i+\frac12}\,dn \to \frac{8}{3}v^{s+1}_{x,i+\frac12}J^{s+1}_{i+\frac12} - \frac{2c}{3\sigma_{a,i+\frac12}}\frac{J^{s+1}_{i+1}-J^{s+1}_i}{\Delta x}, \tag{B.5}$$

$$\varepsilon \int_{-1}^{1} n\widehat{\zeta}_{i+\frac{1}{2}} dn \to \frac{c}{3}(J_{i+1}^{s+1} + J_i^{s+1}). \tag{B.6}$$

In equation (B.3), letting $\varepsilon \to 0$, one can obtain

$$4\pi\sigma_{a,i}\left(\frac{(T_i^{s+1})^4}{4\pi} - J_i^{s+1}\right) = 0.$$

Multiplying equation (B.3) by $\mathcal{P}_0$, adding it to energy equation and substituting limit (B.5) into the equation, then multiplying equation (B.4) by $\frac{\varepsilon}{c}\mathcal{P}_0$, adding it to momentum equation and substituting limit (B.6) into the equation, at last letting $\varepsilon \to 0$ in the two equations, one can obtain

$$\begin{aligned} a\frac{(\rho T)_i^{s+1} - (\rho T)_i^s}{\Delta t} &+ \frac{(\rho v^2 + B^2)_i^{s+1} - (\rho v^2 + B^2)_i^s}{2\Delta t} + \mathcal{P}_0 \frac{(T_i^{s+1})^4 - (T_i^s)^4}{\Delta t} + \frac{1}{\Delta x}(F_{3,i+\frac{1}{2}}^s - F_{3,i-\frac{1}{2}}^s) \\ &+ \frac{4\mathcal{P}_0}{3}\frac{v_{x,i+\frac{1}{2}}^{s+1}(T_{i+\frac{1}{2}}^{s+1})^4 - v_{x,i-\frac{1}{2}}^{s+1}(T_{i-\frac{1}{2}}^{s+1})^4}{\Delta x} = \frac{\mathcal{P}_0 c}{3\sigma_{a,i+\frac{1}{2}}\Delta x}\frac{(T_{i+1}^{s+1})^4 - (T_i^{s+1})^4}{\Delta x} - \frac{\mathcal{P}_0 c}{3\sigma_{a,i-\frac{1}{2}}\Delta x}\frac{(T_i^{s+1})^4 - (T_{i-1}^{s+1})^4}{\Delta x}, \end{aligned} \tag{B.7}$$

$$\frac{(\rho v_x)_i^{s+1} - (\rho v_x)_i^s}{\Delta t} + \frac{1}{\Delta x}(F_{2,i+\frac{1}{2}}^s - F_{2,i-\frac{1}{2}}^s) + \frac{\mathcal{P}_0}{6}\frac{(T_{i+1}^{s+1})^4 - (T_{i-1}^{s+1})^4}{\Delta x} = 0, \tag{B.8}$$

which are fully discretization for (2.14c) and (2.14b).

References

[1] Simon Bolding, Joshua Hansel, Jarrod D. Edwards, Jim E. Morel, and Robert B. Lowrie, *Second-order discretization in space and time for radiation-hydrodynamics*, Journal of Computational Physics **338** (2017), 511 –526.

[2] Moysey Brio and Cheng Chin Wu, *An upwind differencing scheme for the equations of ideal magnetohydrodynamics*, Journal of computational physics **75** (1988), no. 2, 400–422.

[3] Francis Filbet and Shi Jin, *A class of asymptotic-preserving schemes for kinetic equations and related problems with stiff sources*, Journal of Computational Physics **229** (2010), no. 20, 7625–7648.

[4] Pauline Godillon-Lafitte and Thierry Goudon, *A coupled model for radiative transfer: Doppler effects, equilibrium, and nonequilibrium diffusion asymptotics*, Multiscale Modeling & Simulation **4** (2005), no. 4, 1245–1279.

[5] François Golse, Shi Jin, and C David Levermore, *The convergence of numerical transfer schemes in diffusive regimes i: Discrete-ordinate method*, SIAM journal on numerical analysis **36** (1999), no. 5, 1333–1369.

[6] Yan-Fei Jiang, James M. Stone, and Shane W. Davis, *A godunov method for multidimensional radiation magnetohydrodynamics based on a variable eddington tensor*, The Astrophysical Journal Supplement Series **199** (2012), no. 1, 14.

[7] Yan-Fei Jiang, James M. Stone, and Shane W. Davis, *An algorithm for radiation magnetohydrodynamics based on solving the time-dependent transfer equation*, The Astrophysical Journal Supplement Series **213** (2014), no. 1, 7.

[8] Shi Jin, *Efficient asymptotic-preserving (ap) schemes for some multiscale kinetic equations*, SIAM Journal on Scientific Computing **21** (1999), no. 2, 441–454.

[9] Shi Jin, *Asymptotic preserving (ap) schemes for multiscale kinetic and hyperbolic equations* (2010).

[10] Shi Jin and C David Levermore, *Fully-discrete numerical transfer in diffusive regimes*, Transport theory and statistical physics **22** (1993), no. 6, 739–791.

[11] Shi Jin, Lorenzo Pareschi, and Giuseppe Toscani, *Diffusive relaxation schemes for multiscale discrete-velocity kinetic equations*, SIAM Journal on Numerical Analysis **35** (1998), no. 6, 2405–2439.

[12] Shi Jin, Min Tang, and Houde Han, *A uniformly second order numerical method for the one-dimensional discrete-ordinate transport equation and its diffusion limit with interface*, Networks & Heterogeneous Media **4** (2009), no. 1, 35.

[13] Samet Y. Kadioglu, Dana A. Knoll, Robert B. Lowrie, and Rick M. Rauenzahn, *A second order self-consistent imex method for radiation hydrodynamics*, Journal of Computational Physics **229** (2010), no. 22, 8313 –8332.

[14] Axel Klar, *An asymptotic-induced scheme for nonstationary transport equations in the diffusive limit*, SIAM journal on numerical analysis **35** (1998), no. 3, 1073–1094.

[15] Kerstin Küpper, Martin Frank, and Shi Jin, *An asymptotic preserving two-dimensional staggered grid method for multiscale transport equations*, SIAM Journal on Numerical Analysis **54** (2016), no. 1, 440–461.

[16] Edward W Larsen and Jim E Morel, *Asymptotic solutions of numerical transport problems in optically thick, diffusive regimes ii* (1989).

[17] Edward W Larsen, Jim E Morel, and Warren F Miller Jr, *Asymptotic solutions of numerical transport problems in optically thick, diffusive regimes*, Journal of Computational Physics **69** (1987), no. 2, 283–324.

[18] Fengyan Li, Liwei Xu, and Sergey Yakovlev, *Central discontinuous galerkin methods for ideal mhd equations with the exactly divergence-free magnetic field*, Journal of Computational Physics **230** (2011), no. 12, 4828–4847.

[19] RB Lowrie, JE Morel, and JA Hittinger, *The coupling of radiation and hydrodynamics*, The astrophysical journal **521** (1999), no. 1, 432.

[20] Robert B Lowrie and Jarrod D Edwards, *Radiative shock solutions with grey nonequilibrium diffusion*, Shock Waves **18** (2008), no. 2, 129–143.

[21] Ryan G. McClarren, Thomas M. Evans, Robert B. Lowrie, and Jeffery D. Densmore, *Semi-implicit time integration for pn thermal radiative transfer*, Journal of Computational Physics **227** (2008), no. 16, 7561 –7586.

[22] Luc Mieussens, *On the asymptotic preserving property of the unified gas kinetic scheme for the diffusion limit of linear kinetic models*, Journal of Computational Physics **253** (2013), 138–156.

[23] D Mihalas and BW Mihalas, *Foundations of radiation hydrodynamics oxford university press*, New York (1984).

[24] J.E. Morel, Todd A. Wareing, and Kenneth Smith, *A linear-discontinuous spatial differencing scheme forsnradiative transfer calculations*, Journal of Computational Physics **128** (1996), no. 2, 445 –462.

[25] Gerald C Pomraning, *The equations of radiation hydrodynamics*, Courier Corporation, 2005.

[26] Philip L Roe, *Characteristic-based schemes for the euler equations*, Annual review of fluid mechanics **18** (1986), no. 1, 337–365.

[27] Michael Sekora and James Stone, *A higher-order godunov method for radiation hydrodynamics: Radiation subsystem*, Communications in Applied Mathematics and Computational Science **4** (2009), no. 1, 135–152.

[28] Michael D. Sekora and James M. Stone, *A hybrid godunov method for radiation hydrodynamics*, Journal of Computational Physics **229** (2010), no. 19, 6819 –6852.

[29] James M Stone, Thomas A Gardiner, Peter Teuben, John F Hawley, and Jacob B Simon, *Athena: a new code for astrophysical mhd*, The Astrophysical Journal Supplement Series **178** (2008), no. 1, 137.

[30] Wenjun Sun, Song Jiang, and Kun Xu, *An asymptotic preserving unified gas kinetic scheme for gray radiative transfer equations*, Journal of Computational Physics **285** (2015), 265–279.

[31] Wenjun Sun, Song Jiang, Kun Xu, and Guiyu Cao, *Multiscale simulation for the system of radiation hydrodynamics*, Journal of Scientific Computing **85** (2020), no. 2, 1–24.

School of Mathematics, Institute of Natural Sciences and MOE-LSC, Shanghai Jiao Tong University, China
Email address: shijin-m@sjtu.edu.cn

School of Mathematics, Institute of Natural Sciences and MOE-LSC, Shanghai Jiao Tong University, China
Email address: tangmin@sjtu.edu.cn

School of Mathematics, Institute of Natural Sciences and MOE-LSC, Shanghai Jiao Tong University, China
Email address: xjzhang123@sjtu.edu.cn